

Tradeoffs between convergence rate and noise amplification for momentum-based accelerated optimization algorithms

Hesameddin Mohammadi, Meisam Razaviyayn, and Mihailo R. Jovanović

Abstract

We study momentum-based first-order optimization algorithms in which the iterations utilize information from the two previous steps and are subject to an additive white noise. This class of algorithms includes heavy-ball and Nesterov's accelerated methods as special cases. For strongly convex quadratic problems, we use the steady-state variance of the error in the optimization variable to quantify noise amplification and exploit a novel geometric viewpoint to establish analytical lower bounds on the product between the settling time and the smallest/largest achievable noise amplification. For all stabilizing parameters, these bounds scale quadratically with the condition number. We also use the geometric insight developed in the paper to introduce two parameterized families of algorithms that strike a balance between noise amplification and settling time while preserving order-wise Pareto optimality. Finally, for a class of continuous-time gradient flow dynamics, whose suitable discretization yields two-step momentum algorithm, we establish analogous lower bounds that also scale quadratically with the condition number.

Index Terms

First-order algorithms, convergence rate, convex optimization, heavy-ball method, noise amplification, Nesterov's accelerated algorithm, performance tradeoffs, settling time.

I. INTRODUCTION

Accelerated first-order algorithms [1]–[3] are often used for solving large-scale optimization problems [4]–[6] because of their fast convergence, low per-iteration complexity, and favorable scalability. Convergence properties of these algorithms have been carefully studied [7]–[12], but their performance in the presence of noise has received less attention [13]–[15]. Prior studies indicate that inaccuracies in the computation of gradient values can adversely impact the convergence rate of accelerated methods and that gradient descent may have advantages relative to its accelerated variants in noisy environments [16]–[21].

Control-theoretic tools were employed in [21] to quantify robustness to additive white noise of popular first-order algorithms for strongly convex problems. For the parameters that optimize convergence rates for quadratic problems, tight upper and lower bounds on the noise amplification of gradient descent, heavy-ball method, and Nesterov's accelerated algorithms were developed [21]. These bounds are expressed in terms of the condition number κ and the problem dimension n , and they demonstrate opposite trends relative to the settling time: for a fixed problem dimension n , accelerated algorithms increase noise amplification by a factor of $\Theta(\sqrt{\kappa})$ relative to gradient descent. Similar result also holds for heavy-ball and Nesterov's algorithms with parameters that provide convergence rate $\rho \leq 1 - c/\sqrt{\kappa}$ with $c > 0$ [21]. Furthermore, for all strongly convex optimization problems with a condition number κ , tight and attainable upper bounds for noise amplification of gradient descent and Nesterov's accelerated method were provided [21].

In contrast to gradient descent, asymptotically stable accelerated algorithms can also exhibit undesirable transient behavior [22]. Recently, the tools from control theory were used to quantify transient responses for convex quadratic problems and to establish an upper bound on the largest value of the Euclidean distance between the optimization variable and the global minimizer for general strongly convex problems [23]. This upper bound scales as the square root of the condition number and there are quadratic problems for which accelerated algorithms generate transient responses which are within a constant factor of this upper bound [23].

In this paper, we extend the results of [21] to the class of first-order algorithms with three constant parameters in which the iterations involve information from the two previous steps. This class of algorithms includes heavy-ball and Nesterov's accelerated schemes as special cases and we examine its stochastic performance for strongly convex quadratic problems. Our results are complementary to [24], which evaluates stochastic performance in the

Financial support from the National Science Foundation under Awards ECCS 1708906 and ECCS 1809833 is gratefully acknowledged.

Hesameddin Mohammadi and Mihailo R. Jovanović are with the Ming Hsieh Department of Electrical and Computer Engineering, University of Southern California, Los Angeles, CA 90089, USA. (e-mail: hesamedm@usc.edu; mihailo@usc.edu). Meisam Razaviyayn is with the Daniel J. Epstein Department of Industrial and Systems Engineering, University of Southern California, Los Angeles, CA 90089, USA (e-mail: razaviya@usc.edu).

objective error, and to recent work [25], which combines theoretical developments with computational experiments to demonstrate that a parameterized family of heavy-ball-like methods with reduced stepsize provides Pareto-optimal algorithms for simultaneous optimization of noise amplification and convergence rate. In contrast to [25], we establish an analytical lower bound on the product of the settling time and the noise amplification of two-step momentum method for any stabilizing algorithmic parameters. This lower bound scales with the square of the condition number and it reveals a fundamental limitation of this class of algorithms with constant stabilizing parameters.

Our results built upon a simple, yet powerful geometric viewpoint, which clarifies the relation between condition number, convergence rate, and algorithmic parameters for strongly convex quadratic problems. This allows us to present novel alternative proofs for (i) the optimal convergence rate of the two-step momentum algorithm, which recovers Nesterov’s fundamental lower bound on the convergence rate [26]; and (ii) the optimal rates achieved by the special cases of standard gradient descent, heavy-ball method, and Nesterov’s accelerated algorithms [10]. In addition, this viewpoint enables a novel geometric characterization of noise amplification in terms of stability margins and allows us to precisely quantify tradeoffs between convergence rate and robustness to noise.

We also introduce two parameterized families of algorithms that are structurally similar to the heavy-ball and Nesterov’s accelerated algorithms. These algorithms utilize continuous transformations to transition from gradient descent to the corresponding accelerated algorithm (with the optimal convergence rate) via a homotopy path, and they can be used to provide additional insight into the tradeoff between convergence rate and noise amplification. We prove that these parameterized families of algorithms are order-wise (in terms of the condition number) Pareto-optimal for simultaneous minimization of settling time and noise amplification. Another family of algorithms that facilitates similar tradeoff was proposed in [11], and this family includes the fastest known algorithm for the class of smooth strongly convex problems.

Finally, we examine noise amplification of a class of stochastically-forced momentum-based accelerated gradient flow dynamics. Such dynamics were introduced in [27] as a continuous-time variant of Nesterov’s accelerated algorithm and a Lyapunov-based method was utilized to establish their stability properties and infer the convergence rate. Inspired by this work, we examine the tradeoffs between the noise amplification and convergence rate of similar gradient flow dynamics for strongly convex quadratic problems. We introduce a geometric viewpoint analogous to the discrete-time setting and use it to characterize the optimal convergence rate along with the corresponding algorithmic parameters. We then provide a complete characterization of the noise amplification in terms of the parameters and the spectrum of the Hessian matrix. We demonstrate that our findings from the discrete-time setup extend to the continuous-time case as well.

The rest of the paper is organized as follows. In Section II, we provide preliminaries and background material and, in Section III, we summarize our key contributions. In Section IV, we introduce the tools and ideas that enable our analysis. In particular, we utilize the Jury stability criterion to provide novel geometric characterization of stability and ρ -linear convergence and exploit this insight to derive alternative proofs of standard convergence results and quantify fundamental stochastic performance tradeoffs. In Section V, we introduce two parameterized families of algorithms that allow us to constructively tradeoff settling time and noise amplification. In Section VI, we extend our results to the continuous-time setting, in Section VII, we provide proofs of our main results, and in Section VIII, we conclude the paper with remarks.

II. PRELIMINARIES AND BACKGROUND

For unconstrained optimization problems

$$\underset{x}{\text{minimize}} \ f(x) \quad (1)$$

where $f: \mathbb{R}^n \rightarrow \mathbb{R}$ is a strongly convex function with a Lipschitz continuous gradient ∇f , we consider noisy momentum-based first-order algorithms in which information from the two previous steps is used to update the optimization variable x^t ,

$$x^{t+2} = x^{t+1} + \beta(x^{t+1} - x^t) - \alpha \nabla f(x^{t+1} + \gamma(x^{t+1} - x^t)) + \sigma w^t. \quad (2)$$

Here, t is the iteration index, α is the stepsize, β and γ are momentum parameters used for acceleration, σ is the noise magnitude, and w^t is an additive white noise with zero mean and identity covariance matrix,

$$\mathbb{E}[w^t] = 0, \quad \mathbb{E}[w^t(w^\tau)^T] = I \delta(t - \tau)$$

where δ is the Kronecker delta and \mathbb{E} is the expected value. If the only source of uncertainty is a noisy gradient, we set $\sigma = \alpha\sigma_a$ in (2) to account for the effect of stepsize on the noise magnitude; otherwise we set $\sigma = \sigma_a$, where σ_a denotes the actual noise magnitude. Special cases of (2) include noisy gradient descent ($\beta = \gamma = 0$), Polyak's heavy-ball method ($\gamma = 0$), and Nesterov's accelerated algorithm ($\gamma = \beta$).

In the absence of noise (i.e., for $\sigma = 0$), the parameters (α, β, γ) can be selected such that the iterates converge to the globally optimal solution x^* of (1) at a linear rate ρ ,

$$\|z^t\| \leq c \rho^t \max\{\|z^1\|, \|z^0\|\} \quad \text{for all } t \geq 1$$

where $z^t := x^t - x^*$ is the distance to the optimal solution and c is a positive scalar. For the family of smooth strongly convex problems, the parameters that yield the fastest known linear convergence rate were provided in [12]; this reference introduced an additional term $y^t = x^t + \eta(x^t - x^{t-1})$ for evaluation of the error in the objective function $f(y^t)$ and the resulting algorithm was called a *triple momentum algorithm*.

A. Linear dynamics for quadratic problems

Let \mathcal{Q}_m^L denote the class of m -strongly convex L -smooth quadratic functions

$$f(x) = \frac{1}{2} x^T Q x - q^T x \quad (3)$$

with the condition number $\kappa := L/m$, where q is a vector and $Q = Q^T \succ 0$ is the Hessian matrix with eigenvalues

$$L = \lambda_1 \geq \lambda_2 \geq \dots \geq \lambda_n = m > 0.$$

For the quadratic objective function in (3), we can use a linear time-invariant (LTI) state-space model to describe the *two-step momentum algorithm* (2) with constant parameters (α, β, γ) ,

$$\begin{aligned} \psi^{t+1} &= A \psi^t + B w^t \\ z^t &= C \psi^t \end{aligned} \quad (4a)$$

where ψ^t is the state, $z^t := x^t - x^*$ is the performance output, and w^t is the white stochastic input. In particular, choosing $\psi^t := [(x^t - x^*)^T (x^{t+1} - x^*)^T]^T$ yields

$$\begin{aligned} A &= \begin{bmatrix} 0 & I \\ -\beta I + \gamma \alpha Q & (1 + \beta)I - (1 + \gamma)\alpha Q \end{bmatrix} \\ B^T &= [0 \quad \sigma I], \quad C = [I \quad 0]. \end{aligned} \quad (4b)$$

B. Convergence rates

We call an algorithm stable if in the absence of noise (i.e., $\sigma = 0$), the state converges linearly with some rate $\rho < 1$,

$$\|\psi^t\| \leq c \rho^t \|\psi^0\| \quad \text{for all } t \geq 1 \quad (5)$$

for all functions $f \in \mathcal{Q}_m^L$, where $c > 0$ is a constant. For LTI system (4a), the spectral radius $\rho(A)$ of the matrix A determines the best achievable convergence rate.

For the class \mathcal{Q}_m^L of infinite dimensional functions (i.e., for $n = \infty$), Nesterov established the fundamental lower bound on the convergence rate of any first-order algorithm [9],

$$\frac{1}{1 - \rho} \geq \frac{\sqrt{\kappa} + 1}{2}. \quad (6)$$

The quantity $1/(1 - \rho)$ determines the *settling time*, i.e., the number of iterations required to reach a given desired accuracy; see Appendix A. This lower bound is sharp and it is achieved by the heavy-ball method with the parameters provided in Table I [10].

C. Noise amplification

For LTI system (4a) driven by an additive white noise w^t , $\mathbb{E}(\psi^{t+1}) = A \mathbb{E}(\psi^t)$. Thus, $\mathbb{E}(\psi^t) = A^t \mathbb{E}(\psi^0)$ and, for any stabilizing parameters (α, β, γ) , the iterates reach a statistical steady-state with $\lim_{t \rightarrow \infty} \mathbb{E}(\psi^t) = 0$ and a variance that can be computed from the solution of the algebraic Lyapunov equation [21], [28]. We call the

method	optimal parameters (α, β, γ)	settling time	noise amplification bounds (J_{\min}, J_{\max})
Gradient	$(\frac{2}{L+m}, 0, 0)$	$(\kappa + 1)/2$	$(\sigma^2(\Theta(\kappa) + n), \sigma^2 n \Theta(\kappa))$
Nesterov	$(\frac{4}{3L+m}, \frac{\sqrt{3\kappa+1}-2}{\sqrt{3\kappa+1}+2}, \frac{\sqrt{3\kappa+1}-2}{\sqrt{3\kappa+1}+2})$	$\sqrt{3\kappa+1}/2$	$(\sigma^2(\Theta(\kappa\sqrt{\kappa}) + n), \sigma^2 n \Theta(\kappa\sqrt{\kappa}))$
Heavy-ball	$(\frac{4}{(\sqrt{L} + \sqrt{m})^2}, \frac{(\sqrt{\kappa}-1)^2}{(\sqrt{\kappa}+1)^2}, 0)$	$(\sqrt{\kappa} + 1)/2$	$(\sigma^2(\Theta(\kappa\sqrt{\kappa}) + n\Theta(\sqrt{\kappa})), \sigma^2 n \Theta(\kappa\sqrt{\kappa}))$

Table I

SETTLING TIMES $1/(1 - \rho)$ [10, PROPOSITION 1] ALONG WITH THE CORRESPONDING NOISE AMPLIFICATION BOUNDS [21, THEOREM 4] FOR THE PARAMETERS THAT OPTIMIZE THE LINEAR CONVERGENCE RATE ρ FOR STRONGLY CONVEX QUADRATIC FUNCTION $f \in \mathcal{Q}_m^L$ WITH THE CONDITION NUMBER $\kappa := L/m$. HERE, n IS THE PROBLEM DIMENSION ($x \in \mathbb{R}^n$) AND σ^2 IS THE VARIANCE OF THE WHITE NOISE.

steady-state variance of the error in the optimization variable noise amplification (or variance amplification),

$$J := \lim_{t \rightarrow \infty} \frac{1}{t} \sum_{k=0}^t \mathbb{E}(\|x^k - x^*\|^2). \quad (7)$$

In addition to the algorithmic parameters (α, β, γ) , the entire spectrum $\{\lambda_i \mid i = 1, \dots, n\}$ of the Hessian matrix Q impacts the noise amplification J of algorithm (2) [21].

Remark 1: An alternative performance metric that examines the steady-state variance of $y^t - x^*$ was considered in [25], where $y^t := x^t + \gamma(x^t - x^{t-1})$ is the point at which the gradient is evaluated in (2). Since $J_x \leq J_y \leq (1 + 2|\gamma|)^2 J_x$ for all γ , where the subscripts x and y denote the noise amplification in terms of the error in x^t and y^t , these performance metrics are within a constant factor of each other for bounded values of γ .

D. Parameters that optimize convergence rate

For special instances of two-step momentum algorithm (2), namely gradient descent (gd), heavy-ball method (hb), and Nesterov's accelerated algorithm (na), the parameters that optimize the convergence rates are given in [10, Proposition 1]. These parameters along with the corresponding rates and the noise amplification bounds are provided in Table I. The convergence rates are determined by the spectral radius of the corresponding A -matrices and the noise amplification bounds are computed by examining the solution to the algebraic Lyapunov equation and determining the functions $f \in \mathcal{Q}_m^L$ for which the steady-state variance is maximized/minimized [21, Proposition 1]. Since the optimal convergence rate for the heavy-ball method meets the fundamental lower bound (6), this choice of parameters also optimizes the convergence rate of the two-step momentum algorithm (2) for $f \in \mathcal{Q}_m^L$.

For the optimal parameters provided in Table I, there is a $\Theta(\sqrt{\kappa})$ improvement in settling times of the heavy-ball and Nesterov's accelerated algorithms relative to gradient descent,

$$\frac{1}{1 - \rho} = \begin{cases} \Theta(\kappa) & \text{gd} \\ \Theta(\sqrt{\kappa}) & \text{hb, na} \end{cases} \quad (8)$$

where $a = \Theta(b)$ means that a lies within constant factors of b as $b \rightarrow \infty$. This improvement makes accelerated algorithms popular for problems with large condition number κ .

In contrast to the convergence rate, the entire spectrum of Q influences noise amplification and its smallest and largest values over the class of strongly convex quadratic functions,

$$J_{\min} := \min_{f \in \mathcal{Q}_m^L} J, \quad J_{\max} := \max_{f \in \mathcal{Q}_m^L} J \quad (9)$$

depend on the noise magnitude σ , the algorithmic parameters (α, β, γ) , the problem dimension n , and the extreme eigenvalues m and L of Q . For the parameters that optimize convergence rates, tight upper and lower bounds on the noise amplification were developed in [21, Theorem 4]. These bounds are expressed in terms of the condition number κ and the problem dimension n , and they demonstrate opposite trends relative to the settling time. In

particular, for gradient descent,

$$J_{\min} = \sigma^2(\Theta(\kappa) + n), \quad J_{\max} = \sigma^2 n \Theta(\kappa) \quad (10a)$$

and for accelerated algorithms,

$$\begin{aligned} J_{\min} &= \begin{cases} \sigma^2(\Theta(\kappa\sqrt{\kappa}) + n\Theta(\sqrt{\kappa})) & \text{hb} \\ \sigma^2(\Theta(\kappa\sqrt{\kappa}) + n) & \text{na} \end{cases} \\ J_{\max} &= \sigma^2 n \Theta(\kappa\sqrt{\kappa}). \end{aligned} \quad (10b)$$

Thus, for fixed problem dimension n and noise magnitude σ , accelerated algorithms increase noise amplification by a factor of $\Theta(\sqrt{\kappa})$ relative to gradient descent for the parameters that optimize convergence rates. While similar result also holds for heavy-ball and Nesterov's algorithms with arbitrary values of parameters α and β that provide convergence rate $\rho \leq 1 - c/\sqrt{\kappa}$ with $c > 0$ [21, Theorem 8], in this paper we establish the existence of a fundamental tradeoff between noise amplification and settling time for the two-step momentum method (2) with arbitrary stabilizing values of constant parameters (α, β, γ) .

III. SUMMARY OF MAIN RESULTS

In this section, we summarize our key contributions regarding robustness/convergence tradeoff for noisy two-step momentum algorithm (2). A novel geometric characterization of conditions for stability and ρ -linear convergence, developed in Section IV, allows us to provide alternative proofs of standard convergence results and quantify fundamental performance tradeoffs. We first provide an upper bound on noise amplification J in terms of the stability margin $1 - \rho$ and then derive tight upper and lower bounds on the best achievable values of $J_{\min}/(1 - \rho)$ and $J_{\max}/(1 - \rho)$, where J_{\min} and J_{\max} are defined in (9).

A. Bounded noise amplification for stabilizing parameters

For a discrete-time LTI system with a convergence rate ρ , the distance of the eigenvalues to the unit circle is larger than $1 - \rho$. We use this stability margin to establish an upper bound on the noise amplification J of the two-step momentum method (2) for *any* stabilizing parameters (α, β, γ) .

Theorem 1: Let the parameters (α, β, γ) be such that the two-step momentum algorithm (2) converges linearly with the rate $\rho < 1$ for all $f \in \mathcal{Q}_m^L$. Then,

$$J \leq \frac{\sigma^2 n (1 + \rho^2)}{(1 + \rho)^3 (1 - \rho)^3} \quad (11a)$$

where n is the problem size. Furthermore, if $\sigma = \alpha \sigma_a$, i.e., when the only source of uncertainty is a noisy gradient,

$$J \leq \frac{\sigma_a^2 n (1 + \rho)(1 + \rho^2)}{L^2 (1 - \rho)^3}. \quad (11b)$$

For $\rho < 1$, upper bounds in (11) are increasing functions of ρ that become unbounded as $\rho \rightarrow 1$. In addition, both upper bounds are *exact* and they can be achieved by the heavy-ball method with the parameters that optimize the convergence rate (see Table I). We note that bounds in (11) are not tight for all stabilizing parameters. For example, applying (11a) to gradient descent with the optimal stepsize $\alpha = 2/(L + m)$ yields $J \leq \sigma^2 n \Theta(\kappa^3)$; this bound is off by a factor of κ^2 ; cf. Table I. Finally, as we demonstrate in Section VII, the bound in (11b) is obtained by combining (11a) with $\alpha L \leq (1 + \rho)^2$.

B. Tradeoff between settling time and noise amplification

For a fixed condition number κ and a problem size n , we are interested in designing parameters (α, β, γ) to simultaneously minimize settling time $1/(1 - \rho)$ and noise amplification J . As noted in Section II, such a design may involve a tradeoff between these quantities. Since J depends on the entire spectrum of the Hessian matrix Q , we study this tradeoff by examining the smallest and largest values of J over the function class \mathcal{Q}_m^L (i.e., J_{\min} and J_{\max} defined in (9)). We prove that the Pareto front for minimizing either J_{\min} or J_{\max} vs the settling time $1/(1 - \rho)$ can be characterized by explicit upper and lower bounds on $J_{\min}/(1 - \rho)$ and $J_{\max}/(1 - \rho)$. These bounds scale quadratically with κ .

Theorem 2: Let the parameters (α, β, γ) be such that the two-step momentum algorithm (2) converges linearly with the rate $\rho < 1$ for all $f \in \mathcal{Q}_m^L$. Then, J_{\min} and J_{\max} in (9) satisfy,

$$\frac{J_{\min}}{1 - \rho} \geq \sigma^2 \left(\frac{\kappa^2}{64} + (n - 1) \frac{\sqrt{\kappa} + 1}{2} \right) \quad (12a)$$

$$\frac{J_{\max}}{1 - \rho} \geq \sigma^2 \left((n - 1) \frac{\kappa^2}{64} + \frac{\sqrt{\kappa} + 1}{2} \right). \quad (12b)$$

Furthermore, for $\sigma = \alpha\sigma_a$, i.e., when the only source of uncertainty is a noisy gradient, we have

$$\begin{aligned} \frac{J_{\min}}{1 - \rho} &\geq \frac{\sigma_a^2}{L^2} \left(\frac{\kappa^2}{4} + (n - 1) \max \left\{ (1 - \rho)^3 \kappa^2, \frac{1}{4} \right\} \right) \\ \frac{J_{\max}}{1 - \rho} &\geq \frac{\sigma_a^2}{L^2} \left((n - 1) \frac{\kappa^2}{4} + \max \left\{ (1 - \rho)^3 \kappa^2, \frac{1}{4} \right\} \right). \end{aligned}$$

Since the lower bounds in (12) hold for any stabilizing parameters, they also hold for the Pareto fronts that are obtained by minimizing J_{\min} and J_{\max} over (α, β, γ) ; see Figure 1 for an illustration. These bounds scale as $\Theta(\kappa^2)$ when the problem dimension n is fixed. Theorem 3 establishes $\Theta(\kappa^2)$ upper bounds and demonstrates the tightness of this scaling.

Theorem 3: For the class of functions \mathcal{Q}_m^L with condition number $\kappa = L/m$, let the scalar ρ be such that

$$1/(1 - \rho) \in [(\sqrt{\kappa} + 1)/2, (\kappa + 1)/2].$$

Then, we can select parameters $\alpha \geq 1/L$ and β such that the two-step momentum algorithm (2) with $\gamma = 0$ achieves the settling time $1/(1 - \rho)$ and satisfies

$$J_{\min}/(1 - \rho) \leq \sigma^2 \kappa (2\kappa + n) \quad (13a)$$

$$J_{\max}/(1 - \rho) \leq \sigma^2 n \kappa (\kappa + 1) \quad (13b)$$

where J_{\min} and J_{\max} are defined in (9).

Theorem 3 establishes $\Theta(\kappa^2)$ upper bounds on $J_{\min}/(1 - \rho)$ and $J_{\max}/(1 - \rho)$ for a parameterized family of heavy-ball-like algorithms with $\gamma = 0$. In these upper bounds, the problem dimension n appears in an additive fashion in (13a) and in a multiplicative fashion in (13b). In addition, the boundaries of the interval for $1/(1 - \rho)$ are determined by the settling times of the heavy-ball method and gradient descent with parameters given in Table I. As we demonstrate in Section V, this result exploits a geometric insight developed in Section IV, which allows us to introduce a continuous transformation between the heavy-ball method and gradient descent. Similar results can also be obtained for a parameterized family of Nesterov-like algorithms with $\gamma = \beta$. For both cases, exact values of parameters along with proofs are presented in Section V.

Figure 1 summarizes our main results. For a fixed condition number κ , the smallest values of J_{\min} and J_{\max} among all stabilizing parameters vs the settling time (black curves) are lower bounded by (12a) and (12b) (dashed red curves), and upper bounded by (13a) and (13b) (orange curves), respectively. For a fixed problem dimension n all four bounds scale as $\Theta(\kappa^2)$ and they are tight up to constant factors. The general upper bound on J established in Theorem 1 (marked by a blue curve) is exact for the heavy-ball method with the parameters that optimize the settling time, $1/(1 - \rho) = (\sqrt{\kappa} + 1)/2$.

Remark 2: Since \mathcal{Q}_m^L is a subset of the class of m -strongly convex functions with L -Lipschitz continuous gradients, the fundamental lower bounds on $J_{\max}/(1 - \rho)$ established in Theorem 2 carry over to this broader class of problems. Thus, the restriction imposed by the condition number on the tradeoff between settling time and noise amplification goes beyond \mathcal{Q}_m^L and holds for general strongly convex problems.

IV. CONVERGENCE AND NOISE AMPLIFICATION: GEOMETRIC CHARACTERIZATION

In this section, we examine the relation between the convergence rate and noise amplification of the two-step momentum algorithm (2) for strongly convex quadratic problems. In particular, the eigenvalue decomposition of the Hessian matrix Q allows us to bring the dynamics into n decoupled second-order systems parameterized by the eigenvalues of Q and the algorithmic parameters (α, β, γ) . We utilize Jury stability criterion to provide novel geometric characterization of stability and ρ -linear convergence and exploit this insight to derive alternative proofs of standard convergence results and quantify fundamental performance tradeoffs.

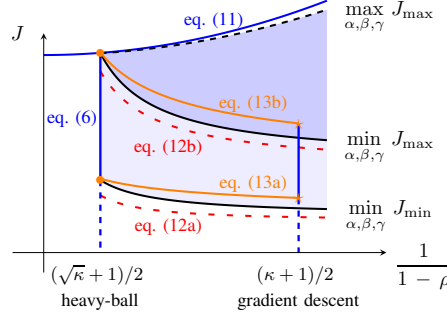


Figure 1. For a fixed condition number κ , the smallest values of $J_{\min} := \min_{f \in \mathcal{Q}_m^L} J$ and $J_{\max} := \min_{f \in \mathcal{Q}_m^L} J$ among all stabilizing parameters vs the settling time (black curves) along with the corresponding lower bounds (12a) and (12b) (dashed red curves), and upper bounds (13a) and (13b) (orange curves). The general upper bound on J established in Theorem 1 is marked by a blue curve.

A. Modal decomposition

We utilize the eigenvalue decomposition of the Hessian matrix $Q = Q^T \succ 0$, $Q = V\Lambda V^T$, where Λ is the diagonal matrix of the eigenvalues and V is the orthogonal matrix of the corresponding eigenvectors. The change of variables $\hat{x}^t := V^T(x^t - x^*)$ and $\hat{w}^t := V^T w^t$ allows us to bring system (4) into n decoupled second-order subsystems,

$$\begin{aligned}\hat{\psi}_i^{t+1} &= \hat{A}_i \hat{\psi}_i^t + \hat{B}_i \hat{w}_i^t \\ \hat{z}_i^t &= \hat{C}_i \hat{\psi}_i^t\end{aligned}\tag{14a}$$

where \hat{w}_i^t is the i th component of the vector $\hat{w}^t \in \mathbb{R}^n$, $\hat{\psi}_i^t = [\hat{x}_i^t \ \hat{x}_i^{t+1}]^T$,

$$\hat{A}_i = \hat{A}(\lambda_i) := \begin{bmatrix} 0 & 1 \\ -a(\lambda_i) & -b(\lambda_i) \end{bmatrix}, \quad \hat{B}_i = \begin{bmatrix} 0 & \sigma \end{bmatrix}^T, \quad \hat{C}_i = \begin{bmatrix} 1 & 0 \end{bmatrix}\tag{14b}$$

and

$$a(\lambda) := \beta - \gamma\alpha\lambda, \quad b(\lambda) := (1 + \gamma)\alpha\lambda - (1 + \beta).\tag{14c}$$

B. Conditions for linear convergence

For the class of strongly convex quadratic functions \mathcal{Q}_m^L , the best convergence rate ρ is determined by the largest spectral radius of the matrices $\hat{A}(\lambda)$ in (14) for $\lambda \in [m, L]$,

$$\rho = \max_{\lambda \in [m, L]} \rho(\hat{A}(\lambda)).\tag{15}$$

For the heavy-ball and Nesterov's accelerated methods, analytical expressions for $\rho(\hat{A}(\lambda))$ were developed and algorithmic parameters that optimize convergences rate were obtained in [10]. Unfortunately, these expressions do not provide insight into the relation between convergence rates and noise amplification.

In this paper, we ask the dual question:

- For a fixed convergence rate ρ , what is the largest condition number κ that can be handled by the two-step momentum algorithm (2) with constant parameters (α, β, γ) ?

We note that the matrices $\hat{A}(\lambda)$ share the same structure as

$$M = \begin{bmatrix} 0 & 1 \\ -a & -b \end{bmatrix}\tag{16a}$$

with the real scalars a and b and that the characteristic polynomial associated with the matrix M is given by

$$F(z) := \det(zI - M) = z^2 + bz + a.\tag{16b}$$

We next utilize the Jury stability criterion [29, Chap. 4-3] to provide conditions for stability of the matrix M given by (16a).

Lemma 1: For the matrix $M \in \mathbb{R}^{2 \times 2}$ given by (16a),

$$\rho(M) < 1 \iff (b, a) \in \Delta \quad (17a)$$

where the stability set

$$\Delta := \{(b, a) \mid |b| - 1 < a < 1\} \quad (17b)$$

is an open triangle in the (b, a) -plane with vertices

$$X = (-2, 1), \quad Y = (2, 1), \quad Z = (0, -1). \quad (17c)$$

Proof: See Appendix C. ■

For any $\rho > 0$, the spectral radius $\rho(M)$ of the matrix M is smaller than ρ if and only if $\rho(M/\rho)$ is smaller than 1. This observation in conjunction with Lemma 1 allow us to obtain necessary and sufficient conditions for stability with the linear convergence rate ρ of the two-step momentum algorithm (2).

Lemma 2: For any positive scalar $\rho < 1$ and the matrix $M \in \mathbb{R}^{2 \times 2}$ given by (16a), we have

$$\rho(M) \leq \rho \iff (b, a) \in \Delta_\rho \quad (18a)$$

where the ρ -linear convergence set

$$\Delta_\rho := \{(b, a) \mid \rho(|b| - \rho) \leq a \leq \rho^2\} \quad (18b)$$

is a closed triangle in the (b, a) -plane with vertices

$$X_\rho = (-2\rho, \rho^2), \quad Y_\rho = (2\rho, \rho^2), \quad Z_\rho = (0, -\rho^2). \quad (18c)$$

Proof: See Appendix C. ■

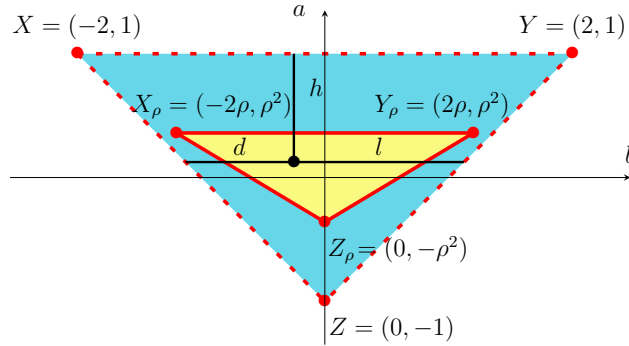


Figure 2. The stability set Δ (the open, cyan triangle) in (17b) and the ρ -linear convergence set Δ_ρ (the closed, yellow triangle) in (18b) along with the corresponding vertices. For the point (b, a) (black bullet) associated with the matrix M in (16a), the corresponding distances (d, h, l) in (23) are marked by black lines.

Figure 2 illustrates the stability and the ρ -linear convergence sets Δ and Δ_ρ , along with their corresponding vertices. We note that for any $\rho \in (0, 1)$, we have $\Delta_\rho \subset \Delta$. This can be verified by observing that the vertices (X_ρ, Y_ρ, Z_ρ) of the triangle Δ_ρ all lie in the triangle Δ . We next use Lemmas 1 and 2 to characterize the convergence rate of the two-step momentum algorithm (2) for strongly convex quadratic problems.

Lemma 3: The two-step momentum algorithm (2) with constant parameters (α, β, γ) is stable for all functions $f \in \mathcal{Q}_m^L$ if and only if the following equivalent conditions hold:

- 1) $(b(\lambda), a(\lambda)) \in \Delta$ for all $\lambda \in [m, L]$;
- 2) $(b(\lambda), a(\lambda)) \in \Delta$ for $\lambda = \{m, L\}$.

Furthermore, the linear convergence rate $\rho < 1$ is achieved for all functions $f \in \mathcal{Q}_m^L$ if and only if the following equivalent conditions hold:

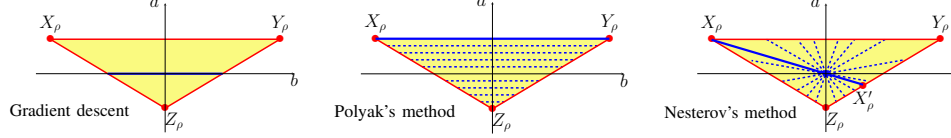


Figure 3. For a fixed ρ -linear convergence triangle Δ_ρ (yellow), dashed blue lines mark the line segments $(b(\lambda), a(\lambda))$ with $\lambda \in [m, L]$ for gradient descent, Polyak's heavy-ball, and Nesterov's accelerated methods as particular instances of the two-step momentum algorithm (2) with constant parameters. The solid blue line segments correspond to the parameters for which the algorithm achieves rate ρ for the largest possible condition number given by (22).

- 1) $(b(\lambda), a(\lambda)) \in \Delta_\rho$ for all $\lambda \in [m, L]$,
- 2) $(b(\lambda), a(\lambda)) \in \Delta_\rho$ for $\lambda = \{m, L\}$.

Here, $(b(\lambda), a(\lambda))$ is given by (14c), and the stability and ρ -linear convergence triangles Δ and Δ_ρ are given by (17b) and (18b), respectively.

Proof: The conditions in 1) follow from combining equation (15) with Lemma 1 (for stability) and with Lemma 2 (for ρ -linear convergence). The conditions in 2) follow from Lemma 3 and the facts that Δ and Δ_ρ are convex sets and that $(b(\lambda), a(\lambda))$ in (14c) is a line segment in the (b, a) -plane with end points corresponding to $\lambda = m$ and $\lambda = L$. ■

Lemma 3 exploits the geometry of the curve $(b(\lambda), a(\lambda))$ in the (b, a) -plane and convexity of the sets Δ and Δ_ρ to establish necessary and sufficient conditions for stability and ρ -linear convergence: the inclusion of the end points of the line segment $(b(\lambda), a(\lambda))$ associated with the extreme eigenvalues m and L of the matrix Q in the corresponding triangle. A similar approach was taken in [25, Appendix A.1], where the affine nature of the conditions resulting from the Jury stability criterion with respect to λ was used to conclude that $\rho(\hat{A}(\lambda))$ is a quasi-convex function of λ and show that the extreme points m and L determine $\rho(A)$. In contrast, we exploit the triangular shapes of the stability and ρ -linear convergence sets Δ and Δ_ρ and utilize this geometric insight to identify the parameters that optimize the convergence rate and to establish tradeoffs between noise amplification and convergence rate.

The following corollary is immediate.

Corollary 1: Let the two-step momentum algorithm (2) with constant parameters (α, β, γ) optimize a function $f \in \mathcal{Q}_m^L$ with a linear rate $\rho < 1$. Then, the convergence rate ρ is achieved for all functions $f \in \mathcal{Q}_m^L$.

Proof: Lemma 3 implies that only the extreme eigenvalues m and L of Q determine ρ . Since all functions $f \in \mathcal{Q}_m^L$ share the same extreme eigenvalues, this completes the proof. ■

For the two-step momentum algorithm (2) with constant parameters, Lemma 3 provides a simple alternative proof for the fundamental lower bound (6) on the settling time established by Nesterov. Our proof utilizes the fact that for any point $(b(\lambda), a(\lambda)) \in \Delta_\rho$, the horizontal signed distance to the edge XZ of the stability triangle Δ satisfies

$$d(\lambda) := a(\lambda) + b(\lambda) + 1 = \alpha\lambda. \quad (19)$$

where a and b are given by (14c); see Figure 2 for an illustration.

Proposition 1: Let the two-step momentum algorithm (2) with constant parameters (α, β, γ) achieve the linear convergence rate $\rho < 1$ for all functions $f \in \mathcal{Q}_m^L$. Then, lower bound (6) on the settling time holds and it is achieved by the heavy-ball method with the parameters provided in Table I.

Proof: Let $d(m) = \alpha m$ and $d(L) = \alpha L$ denote the values of the function $d(\lambda)$ associated with the points $(b(m), a(m))$ and $(b(L), a(L))$, where (b, a) and d are given by (14c) and (19), respectively. Lemma 3 implies that $(b(L), a(L))$ and $(b(m), a(m))$ lie in the ρ -linear convergence triangle Δ_ρ . Thus,

$$d_{\max}/d_{\min} \geq d(L)/d(m) = \kappa$$

where d_{\max} and d_{\min} denote the largest and smallest values that d can take among all points $(b, a) \in \Delta_\rho$. From the shape of Δ_ρ , we conclude that d_{\max} and d_{\min} correspond to the vertices Y_ρ and X_ρ of Δ_ρ given by (18c); see Figure 2. Thus,

$$d_{\max} = d_{Y_\rho} = 1 + \rho^2 + 2\rho = (1 + \rho)^2 \quad (20a)$$

$$d_{\min} = d_{X_\rho} = 1 + \rho^2 - 2\rho = (1 - \rho)^2. \quad (20b)$$

This in conjunction with the previous inequality yields

$$\kappa = \frac{d(L)}{d(m)} \leq \frac{d_{\max}}{d_{\min}} = \left(\frac{1 + \rho}{1 - \rho} \right)^2. \quad (21)$$

Rearranging terms in (21) gives lower bound (6). \blacksquare

To provide additional insight, we next examine the implications of Lemma 3 for gradient descent, Polyak's heavy-ball, and Nesterov's accelerated algorithms. In all three cases, our dual approach recovers the optimal convergence rates provided in Table I. From the definition of a and b in (14c), it follows that the line segment $(b(\lambda), a(\lambda))$ with $\lambda \in [m, L]$ satisfies:

- gradient descent ($\beta = \gamma = 0$): (b, a) is the horizontal line segment parameterized by $a = 0$;
- heavy-ball method ($\gamma = 0$): (b, a) is the horizontal line segment parameterized by $a = \beta$; and
- Nesterov's accelerated method ($\beta = \gamma$): (b, a) is the line segment parameterized by $a = -\beta b / (1 + \beta)$.

These observations are illustrated in Figure 3 and, as we show in the proof of Lemma 3, to obtain the largest possible condition number for which the convergence rate ρ is feasible for each algorithm, one needs to find the largest ratio $d(L)/d(m) = \kappa$ among all possible orientations for the line segment $(b(\lambda), a(\lambda))$ with $\lambda \in [m, L]$ to lie within Δ_ρ . This leads to:

- For gradient descent, the largest ratio $d(L)/d(m)$ corresponds to the intersections of the horizontal axis and the edges $Y_\rho Z_\rho$ and $X_\rho Z_\rho$ of the triangle Δ_ρ , which are given by $(\rho, 0)$ and $(-\rho, 0)$, respectively. Thus, we have

$$\kappa = d(L)/d(m) \leq (1 + \rho)/(1 - \rho). \quad (22a)$$

Rearranging terms in (22a) yields a lower bound on the settling time for gradient descent $1/(1 - \rho) \geq (\kappa + 1)/2$. This lower bound is tight as it can be achieved by choosing the parameters in Table I, which place $(b(\lambda), a(\lambda))$ to $(\rho, 0)$ and $(-\rho, 0)$ for $\lambda = L$ and $\lambda = m$, respectively.

- For the heavy-ball method, the optimal rate is recovered by designing the parameters (α, β) such that the vertices X_ρ and Y_ρ belong to the horizontal line segment $(b(\lambda), a(\lambda))$,

$$\kappa = d(L)/d(m) \leq (1 + \rho)^2/(1 - \rho)^2. \quad (22b)$$

By choosing $d(L) = d_{Y_\rho}$ and $d(m) = d_{X_\rho}$, we recover the optimal parameters provided in Table I and achieve the fundamental lower bound (6) on the convergence rate.

- For Nesterov's accelerated method, the largest ratio $d(L)/d(m)$ corresponds to the line segment $X_\rho X'_\rho$ that passes through the origin, where $X'_\rho = (2\rho/3, -\rho^2/3)$ lies on the edge $Y_\rho Z_\rho$; see Appendix C. This yields

$$\kappa = \frac{d(L)}{d(m)} \leq \frac{1 + 2\rho/3 - \rho^2/3}{(1 - \rho)^2}. \quad (22c)$$

Rearranging terms in this inequality provides a lower bound on the settling time $1/(1 - \rho) \geq \sqrt{3\kappa + 1}/2$. This lower bound is tight and it can be achieved with the parameters provided in Table I, which place $(b(L), a(L))$ to X'_ρ and $(b(m), a(m))$ to X_ρ .

Figure 3 illustrates the optimal orientations discussed above.

C. Noise amplification

To quantify the noise amplification of the two-step momentum algorithm (2), we utilize an alternative characterization of the stability and ρ -linear convergence triangles Δ and Δ_ρ . Let d and l denote the horizontal signed distances of the point (a, b) to the edges XZ and YZ of the stability triangle Δ ,

$$\begin{aligned} d(\lambda) &:= a(\lambda) + b(\lambda) + 1 \\ l(\lambda) &:= a(\lambda) - b(\lambda) + 1. \end{aligned} \quad (23a)$$

and let h denote its vertical signed distance to the edge XY ,

$$h(\lambda) := 1 - a(\lambda). \quad (23b)$$

Then, the following equivalent conditions,

$$(b, a) \in \Delta \iff h, d, l > 0 \quad (24a)$$

$$(b, a) \in \Delta_\rho \iff \begin{cases} h \geq (1 - \rho)(1 + \rho) \\ d \geq (1 - \rho)(1 + \rho + b) \\ l \geq (1 - \rho)(1 + \rho - b) \end{cases} \quad (24b)$$

follow from the definition of the sets Δ in (17b), Δ_ρ in (18b), and (h, d, l) in (23); see Figure 2 for an illustration.

In Theorem 4, we quantify the steady-state variance of the error in the optimization variable in terms of the spectrum of the Hessian matrix and the algorithmic parameters for noisy two-step momentum algorithm (2). Special cases of this result for gradient decent, heavy-ball, and Nesterov's accelerated algorithms were established in [21]. The proof of Theorem 4 follows from similar arguments and we omit it for brevity.

Theorem 4: For a strongly convex quadratic objective function $f \in \mathcal{Q}_m^L$ with the Hessian matrix Q , the steady-state variance of $x^t - x^*$ for the two-step momentum algorithm (2) with any stabilizing parameters (α, β, γ) is determined by

$$J = \sum_{i=1}^n \frac{\sigma^2(d(\lambda_i) + l(\lambda_i))}{2d(\lambda_i)h(\lambda_i)l(\lambda_i)} =: \sum_{i=1}^n \hat{J}(\lambda_i)$$

Here, $\hat{J}(\lambda_i)$ denotes the modal contribution of the i th eigenvalue λ_i of Q to the steady-state variance, (d, h, l) are defined in (23), and (a, b) are given by (14c).

In Appendix G, we describe how the algebraic Lyapunov equation for the steady-state covariance matrix of the error in the optimization variable can be used to compute the noise amplification. Theorem 4 demonstrates that noise amplification J depends on the entire spectrum of the Hessian matrix Q and not only on its extreme eigenvalues m and L , which determine the convergence rate. Since for any $f \in \mathcal{Q}_m^L$ the extreme eigenvalues of Q are fixed at m and L , we have

$$\begin{aligned} J_{\max} &:= \max_{f \in \mathcal{Q}_m^L} J = \hat{J}(m) + \hat{J}(L) + (n - 2)\hat{J}_{\max} \\ J_{\min} &:= \min_{f \in \mathcal{Q}_m^L} J = \hat{J}(m) + \hat{J}(L) + (n - 2)\hat{J}_{\min} \end{aligned}$$

where

$$\hat{J}_{\max} := \max_{\lambda \in [m, L]} \hat{J}(\lambda), \quad \hat{J}_{\min} := \min_{\lambda \in [m, L]} \hat{J}(\lambda).$$

We use these to determine explicit upper and lower bounds on the noise amplification in terms of the condition number.

V. CONSTRUCTING ORDER-WISE PARETO-OPTIMAL ALGORITHMS WITH ADJUSTABLE PARAMETERS

The geometric insight developed in Section IV can be utilized to obtain algorithms that constructively tradeoff settling time and noise amplification via adjustable parameters. In particular, we introduce two parameterized families of momentum-based algorithms that are obtained using *continuous transformations* between the line segments $(b(\lambda), a(\lambda))$, $\lambda \in [m, L]$, associated with gradient descent and Polyak's heavy-ball and Nesterov's accelerated algorithms with the parameters that optimize the convergence rates. For both parameterizations, we establish analytical expressions for $J/(1 - \rho)$ along with tight upper and lower bounds that scale with κ^2 . This is a direct extension of [21, Theorem 4] which focused on the above three standard algorithms but only for the parameters that optimize the corresponding convergence rates. The results established in this section provide a proof for a more detailed version (Proposition 2) of Theorem 3. Furthermore, in conjunction with the lower bounds established in Theorem 2, they characterize order-wise tight upper and lower bounds on the Pareto fronts for minimizing either J_{\max} or J_{\min} vs the settling time.

A. Parameterized family of heavy-ball-like methods

For the two-step momentum algorithm (2) with $\gamma = 0$, $(b(\lambda), a(\lambda))$ is a horizontal line segment in the (b, a) -plane parameterized by $\lambda \in [m, L]$. As described in Section IV, gradient descent and heavy-ball methods with the optimal parameters provided in Table I are obtained for $a = \beta = 0$ and $a = \beta = \rho^2$, respectively, and the corresponding end points $(b(m), a(m))$ and $(b(L), a(L))$ lie on the edges $X_\rho Z_\rho$ and $Y_\rho Z_\rho$ of the ρ -linear convergence triangle Δ_ρ .

To provide a continuous transformation between these two standard algorithms, we introduce a parameter $c \in [0, 1]$, let the line segment satisfy $a = \beta = c\rho^2$, and take its end points at the edges $X_\rho Z_\rho$ and $Y_\rho Z_\rho$; see Figure 3 for an illustration. This can be accomplished with the the following choice of parameters,

$$\alpha = (1 + \rho)(1 + c\rho)/L, \quad \beta = c\rho^2, \quad \gamma = 0. \quad (25)$$

In Lemma 4, we establish expressions for the convergence rate and largest/smallest modal contributions to noise amplification in terms of the condition number for this family of parameters.

Lemma 4: For the class of functions \mathcal{Q}_m^L with the condition number $\kappa = L/m$, let the scalar ρ be such that

$$1/(1 - \rho) \in [(\sqrt{\kappa} + 1)/2, (\kappa + 1)/2].$$

Then, the two-step momentum algorithm (2) with parameters (25) achieves the convergence rate ρ , and the largest and smallest values \hat{J}_{\max} and \hat{J}_{\min} of $\hat{J}(\lambda)$ for $\lambda \in [m, L]$ satisfy

$$\begin{aligned} \hat{J}_{\max} &= \hat{J}(m) = \hat{J}(L) = \frac{\sigma^2(\kappa + 1)}{2(1 - c\rho^2)(1 + \rho)(1 + c\rho)} \\ \hat{J}_{\min} &= \hat{J}(\hat{\lambda}) = \frac{\sigma^2}{1 - c^2\rho^4} \end{aligned}$$

where $\hat{\lambda} := (m + L)/2$ and the scalar c is given by

$$c := \frac{(1 - \rho)\kappa - (1 + \rho)}{\rho((1 - \rho)\kappa + (1 + \rho))} \in [0, 1].$$

Proof: See Appendix D. ■

Lemma 4 allows us to derive analytical expressions for the largest and smallest values that J takes over $f \in \mathcal{Q}_m^L$.

Corollary 2: The parameterized family of heavy-ball-like methods (25) satisfies

$$\begin{aligned} J_{\max} &= n\hat{J}(m) = n\hat{J}(L) \\ J_{\min} &= 2\hat{J}(m) + (n - 2)\hat{J}(\hat{\lambda}) \end{aligned}$$

where $\hat{J}(m)$ and $\hat{J}(\hat{\lambda})$ are given in Lemma 4, and J_{\max} and J_{\min} are the smallest and largest values of J when the algorithm is applied to $f \in \mathcal{Q}_m^L$ with condition number $\kappa = L/m$.

Proof: The result follows from combining Lemma 4, the expression $J = \sum_{i=1}^n \hat{J}(\lambda_i)$ established in Theorem 4, and the fact that J takes its maximum for an objective function f with Q having all the eigenvalues at the extreme points m and L and its minimum for f for which, apart from the extreme eigenvalues m and L , the rest are at $(m + L)/2$. ■

We next establish order-wise tight upper and lower bounds on $\hat{J}_{\max}/(1 - \rho)$ and $\hat{J}_{\min}/(1 - \rho)$ in terms of κ .

Lemma 5: For the parameterized family of heavy-ball-like methods (25), the largest and smallest modal contributions to variance amplification established in Lemma 4 satisfy

$$\begin{aligned} \theta_1 \sigma^2 \kappa (\kappa + 1) &\leq \hat{J}_{\max}/(1 - \rho) \leq \theta_2 \sigma^2 \kappa (\kappa + 1) \\ \theta_3 \sigma^2 \kappa &\leq \hat{J}_{\min}/(1 - \rho) \leq \theta_4 \sigma^2 \kappa \end{aligned}$$

where the scalars $\theta_i \leq 1$ are given by

$$\begin{aligned} \theta_1 &:= (1 + \rho)^{-2}(1 + c\rho)^{-3}/2 \geq 1/64 \\ \theta_2 &:= (1 + \rho)^{-2}(1 + c\rho)^{-2}/2 \geq 1/32 \\ \theta_3 &:= (1 + \rho)^{-1}(1 + c\rho)^{-3} \geq 1/16 \\ \theta_4 &:= (1 + \rho)^{-1}(1 + c\rho^2)^{-2} \geq 1/8. \end{aligned} \quad (26)$$

Proof: See Appendix D. ■

We observe that $\hat{J}_{\max}/(1 - \rho) = \Theta(\kappa^2)$ and $\hat{J}_{\min}/(1 - \rho) = \Theta(\kappa)$. This result also allows us to bound $J/(1 - \rho)$.

Proposition 2: The parameterized family of heavy-ball-like methods (25) satisfies

$$\begin{aligned} J_{\max}/(1-\rho) &\geq \sigma^2 n \theta_1 \kappa (\kappa + 1) \\ J_{\max}/(1-\rho) &\leq \sigma^2 n \theta_2 \kappa (\kappa + 1) \\ J_{\min}/(1-\rho) &\geq \sigma^2 \kappa (2\theta_1(\kappa + 1) + (n-2)\theta_3) \\ J_{\min}/(1-\rho) &\leq \sigma^2 \kappa (2\theta_2(\kappa + 1) + (n-2)\theta_4) \end{aligned}$$

where J_{\max} and J_{\min} are the largest and the smallest values that J can take when the algorithm is applied to $f \in \mathcal{Q}_m^L$ with condition number $\kappa = L/m$ and θ_i 's are given by (26).

Proof: As shown in the proof of Corollary 2, $J/(1-\rho)$ is maximized when the Hessian matrix Q has all the eigenvalues at the extreme points m and L , and it is minimized when, apart from the extreme eigenvalues m and L , the rest are placed at the midpoint. The result follows from the corresponding bounds on $\hat{J}(\lambda)/(1-\rho)$ provided in Lemma 5. ■

B. Parameterized family of Nesterov-like methods

For the two-step momentum algorithm (2) with $\gamma = \beta$, $(b(\lambda), a(\lambda))$ is a line segment parameterized by $\lambda \in [m, L]$ that passes through the origin. As described in Section IV, gradient descent and Nesterov's method with the optimal parameters provided in Table I are obtained for $a = 0$ and $a = -(\rho/2)b$, respectively, and the corresponding end points $(b(m), a(m))$ and $(b(L), a(L))$ lie on the edges $X_\rho Z_\rho$ and $Y_\rho Z_\rho$ of the ρ -linear convergence triangle Δ_ρ . To provide a continuous transformation between these two standard algorithms, we introduce a parameter $c \in [0, 1/2]$, let the line segment satisfy $a = -c\rho b$, and take its end points at the edges $X_\rho Z_\rho$ and $Y_\rho Z_\rho$; see Figure 3 for an illustration. This can be accomplished with the following choice of parameters,

$$\begin{aligned} \alpha &= (1 + \rho)(1 + c - c\rho)/(L(1 + c)) \\ \gamma &= \beta = c\rho^2/((\alpha L - 1)(1 + c)). \end{aligned} \quad (27)$$

In Lemma 6, we establish expressions for the convergence rate and largest/smallest modal contributions to noise amplification in terms of the condition number for this family of parameters.

Lemma 6: For the class of functions \mathcal{Q}_m^L with condition number $\kappa = L/m$, let the scalar ρ be such that $1/(1-\rho) \in [(\sqrt{3\kappa+1})/2, (\kappa+1)/2]$. The two-step momentum algorithm in 2 with parameters (27) achieves the convergence rate ρ , and the extreme values \hat{J}_{\max} and \hat{J}_{\min} of $\hat{J}(\lambda)$ over $[m, L]$ satisfy

$$\begin{aligned} \hat{J}_{\max} = \hat{J}(m) &= \frac{\sigma^2(1-c)^2(r\kappa+1)}{2(1-c-c\rho^2)(1+\rho)(1-c+c\rho)} \\ &\geq \hat{J}(L) = \frac{\sigma^2(1+c)^2(1+c-c\rho^2)}{(1-\rho^2)(1+c-c\rho)(1+c+c\rho)(1+c+c\rho^2)} \end{aligned}$$

and $\hat{J}_{\min} = \hat{J}(1/\alpha) = \sigma^2$, where the scalar $r \in [1, 3]$ is given by $r := (1+c)(1-c+c\rho)/((1-c)(1+c-c\rho))$ and the scalar $c \in [0, 1/2]$ is the solution to the quadratic equation

$$\kappa(1-\rho)(1-c\rho-c^2(1+\rho)) = (1+\rho)(1-c\rho-c^2(1-\rho)).$$

Proof: See Appendix D. ■

Lemma 6 allows us to derive analytical expressions for the largest and smallest values that J takes over $f \in \mathcal{Q}_m^L$.

Corollary 3: The parameterized family of Nesterov-like methods (27) satisfies

$$\begin{aligned} J_{\max} &= (n-1)\hat{J}(m) + \hat{J}(L) \\ J_{\min} &= \hat{J}(m) + \hat{J}(L) + (n-2)\hat{J}(1/\alpha) \end{aligned}$$

where $\hat{J}(m)$, $\hat{J}(L)$, $\hat{J}(1/\alpha)$ are given by Lemma 6, and J_{\max} , J_{\min} are the extreme values of J when the algorithm is applied to $f \in \mathcal{Q}_m^L$ with condition number $\kappa = L/m$.

Proof: The result follows from combining Lemma 6 and the expression $J = \sum_{i=1}^n \hat{J}(\lambda_i)$ established in Theorem 4. In particular, J is maximized when Q has $n-1$ eigenvalues at m and one at L , and it is minimized when, apart from the extreme eigenvalues m and L , the rest are at $\lambda = 1/\alpha$. ■

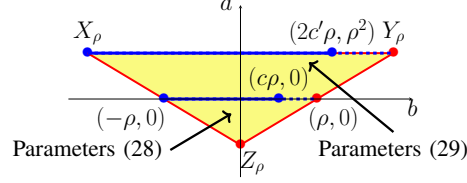


Figure 4. The triangle Δ_ρ (yellow) and the line segments $(b(\lambda), a(\lambda))$ with $\lambda \in [m, L]$ (blue) for gradient descent with reduced stepsize (28) and heavy-ball-like method (29), which place the end point $(b(m), a(m))$ at X_ρ and the end point $(b(L), a(L))$ at $(2c'\rho, \rho^2)$ on the edge $X_\rho Y_\rho$, where $c' := \kappa(1 - \rho)^2/\rho - (1 + \rho^2)/\rho$ ranges over the interval $[-1, 1]$.

We next establish order-wise tight upper and lower bounds on $\hat{J}_{\max}/(1 - \rho)$ and $\hat{J}_{\min}/(1 - \rho)$ in terms of κ .

Lemma 7: For the parameterized family of Nesterov-like methods (27), the largest and smallest modal contributions to variance amplification established in Lemma 6 satisfy

$$\begin{aligned} \sigma^2 \omega_1 r \kappa (r \kappa + 1) &\leq \hat{J}_{\max}/(1 - \rho) \leq \sigma^2 \omega_2 r \kappa (r \kappa + 1) \\ \sigma^2 \sqrt{3\kappa + 1}/2 &\leq \hat{J}_{\min}/(1 - \rho) \leq \sigma^2 (\kappa + 1)/2 \end{aligned}$$

where the scalar $\omega_1 := (1 + \rho)^{-3}(1 - c)^2(1 - c + c\rho)^{-2}/2$, $\omega_2 := (1 + \rho)\omega_1$, and we have $(1 + \rho)^{-5} \leq \omega_1 \leq (1 + \rho)^{-3}$.

Proof: See Appendix D. ■

Similar to the heavy-ball-like methods, $\hat{J}_{\max}/(1 - \rho) = \Theta(\kappa^2)$. However, the upper and lower bounds on $\hat{J}_{\min}/(1 - \rho)$ scale linearly with κ and $\sqrt{\kappa}$, respectively. We next use this result to bound $J/(1 - \rho)$.

Proposition 3: The parameterized family of Nesterov-like methods (27) satisfy

$$\begin{aligned} J_{\max}/(1 - \rho) &\geq \sigma^2 ((n - 1)\omega_1 r \kappa (r \kappa + 1) + \sqrt{3\kappa + 1}/2) \\ J_{\max}/(1 - \rho) &\leq \sigma^2 n \omega_2 r \kappa (r \kappa + 1) \\ J_{\min}/(1 - \rho) &\geq \sigma^2 (\omega_1 r \kappa (r \kappa + 1) + (n - 1)\sqrt{3\kappa + 1}/2) \\ J_{\min}/(1 - \rho) &\leq \sigma^2 (\omega_2 r \kappa (r \kappa + 1) + (n - 1)(\kappa + 1)/2) \end{aligned}$$

where J_{\min} and J_{\max} are the smallest and largest values that J can take when the algorithm is applied to $f \in \mathcal{Q}_m^L$ with condition number $\kappa = L/m$, the scalar $r \in [1, 3]$, and ω_1 and ω_2 are given by Lemmas 6 and 7, respectively.

Proof: As shown in the proof of Corollary 3, $J/(1 - \rho)$ is maximized when Q has $n - 1$ eigenvalues at m and one at L , and is minimized when, apart from the extreme eigenvalues m and L , the rest are placed at $\lambda = 1/\alpha$. Employing the bounds on $\hat{J}_{\max} = \hat{J}(m)$ and $\hat{J}_{\min} = \hat{J}(1/\alpha)$ provided by Lemma 7 and noting that $\hat{J}(L) \in [\hat{J}_{\min}, \hat{J}_{\max}]$ completes the proof. ■

C. Impact of reducing the stepsize

When the only source of uncertainty is a noisy gradient, i.e., $\sigma = \alpha \sigma_a$, one can attempt to reduce the noise amplification J by decreasing the stepsize α at the expense of increasing the settling time $1/(1 - \rho)$. In particular, for gradient descent, α can be reduced from its optimal value $2/(L + m)$ by keeping $(b(m), a(m))$ at $(-\rho, 0)$ and moving the point $(b(L), a(L))$ from $(\rho, 0)$ towards $(-\rho, 0)$ along the horizontal axis; see Figure 4. This can be accomplished with

$$\alpha = (1 + c\rho)/L, \quad \gamma = \beta = 0 \tag{28}$$

for some $c \in [-1, 1]$ parameterizing $(b(L), a(L)) = (c\rho, 0)$. In this case, the settling time satisfies $1/(1 - \rho) = (\kappa + c)/(c + 1) \in [(\kappa + 1/2), \infty)$ and similar arguments to those presented in the proof of Lemma 4 can be used to obtain

$$\begin{aligned} \hat{J}_{\max} &= \hat{J}(m) = \sigma_a^2 \kappa^2 (1 - \rho)/L^2 \\ \hat{J}_{\min} &= \begin{cases} \hat{J}(L) = \sigma_a^2 \alpha^2 / (1 - c^2 \rho^2) & c \leq 0 \\ \hat{J}(1/\alpha) = \sigma_a^2 \alpha^2 & c \geq 0. \end{cases} \end{aligned}$$

For a fixed n , the stepsize in (28) yields a $\Theta(\kappa^2)$ scaling for both $J_{\max}/(1-\rho)$ and $J_{\min}/(1-\rho)$ for all $c \in [-1, 1]$. Thus, gradient descent with reduced stepsize is order-wise close to the lower bounds on Pareto fronts characterized in Theorem 2. An IQC-based approach [21, Lemma 1] was utilized in [25, Theorem 13] to show that stepsize (28) also yields the above discussed convergence rate and worst-case noise amplification for one-point m -strongly convex L -smooth functions.

Remark 3: For any desired settling time $1/(1-\rho) \in [(\sqrt{\kappa}+1)/2, \infty)$, the heavy-ball-like method with reduced stepsize,

$$\alpha = (1-\rho)^2/m, \quad \beta = \rho^2, \quad \gamma = 0 \quad (29)$$

achieves the convergence rate ρ and $J_{\max} = \sigma_a^2 n \kappa^2 (1-\rho^4)/(L^2(1+\rho)^4)$ [25, Theorem 9]; see Figure 4. In addition, by considering the error in $y^t = x^t + \gamma(x^t - x^{t-1})$ as the performance metric, it was stated and numerically verified in [25] that the choice of parameters (29) yields Pareto-optimal algorithms for simultaneously optimizing J_{\max} and ρ . We note that the settling time $1/(1-\rho) = \Theta(\kappa)$ of gradient descent with standard stepsizes ($\alpha = 1/L$ or $2/(m+L)$), by reducing α in (29) to $O(1/(\kappa L))$. In contrast, the parameterized family of heavy-ball-like methods (25) is order-wise Pareto-optimal (cf. Theorems 2 and 3) while maintaining $\alpha \in [1/L, 4/L]$.

VI. CONTINUOUS-TIME GRADIENT FLOW DYNAMICS

Gradient descent with additive noise can be viewed as the forward Euler discretization of gradient flow dynamics (gfd),

$$\dot{x} + \alpha \nabla f(x) = \sigma w \quad (30a)$$

where \dot{x} denotes the derivative of x with respect to time τ and w is a white noise with zero mean and identity covariance matrix, $\mathbb{E}[w(\tau)] = 0$, $\mathbb{E}[w(\tau_1)w^T(\tau_2)] = I\delta(\tau_1 - \tau_2)$. Similarly, noisy two-step momentum algorithm (2) can be obtained by discretizing the accelerated gradient flow dynamics (agd),

$$\ddot{x} + \theta \dot{x} + \alpha \nabla f(x + \gamma \dot{x}) = \sigma w \quad (30b)$$

with $\theta := 1 - \beta$ by approximating x , \dot{x} , and \ddot{x} using

$$x = x^{t+1}, \quad \dot{x} \approx x^{t+1} - x^t, \quad \ddot{x} \approx x^{t+2} - 2x^{t+1} + x^t.$$

System (30b) with $\beta = \gamma$ was introduced in [27] as a continuous-time analogue of Nesterov's accelerated algorithm and a Lyapunov-based method was employed to characterize its stability properties for smooth strongly convex problems.

For a time dilation $s = c\tau$, the solution to (30b) satisfies

$$x'' + \bar{\theta}x' + \bar{\alpha}\nabla f(x + \bar{\gamma}x') = \bar{\sigma}w$$

where $\dot{x} = dx/d\tau$, $x' = dx/ds$, and

$$\bar{\theta} = \theta/c, \quad \bar{\gamma} = c\gamma, \quad \bar{\alpha} = \alpha/c^2, \quad \bar{\sigma} = \sigma/(c\sqrt{c}).$$

This follows by combining $\dot{x} = cx'$ and $\ddot{x} = c^2x''$ with the fact that the time dilation yields a \sqrt{c} increase in the noise magnitude σ . Similar change of variables can be applied to gradient flow dynamics (30a) and to study stability and noise amplification of (30) we set $\alpha = 1/L$ without loss of generality.

A. Modal-decomposition

For quadratic optimization problem (3) with $Q = Q^T \succ 0$, we follow the approach of Section IV-A and utilize the eigenvalue decomposition of $Q = V\Lambda V^T$ and the change of variables, $\hat{x} := V^T(x - x^*)$, $\hat{w} := V^T w$, to bring (30) to,

$$\begin{aligned} \dot{\hat{\psi}}_i &= \hat{A}_i \hat{\psi}_i + \hat{B}_i \hat{w}_i, \\ \hat{z}_i &= \hat{C}_i \hat{\psi}_i \end{aligned} \quad (31a)$$

where \hat{w}_i is the i th component of the vector \hat{w} . For gradient flow dynamics (30a), we let $\hat{\psi}_i := \hat{x}_i$, which leads to

$$\hat{A}_i = -\alpha\lambda_i =: -a(\lambda_i), \quad \hat{B}_i = \sigma, \quad \hat{C}_i = 1. \quad (31b)$$

On the other hand, for accelerated gradient flow dynamics (30b), $\hat{\psi}_i := [\hat{x}_i \quad \dot{\hat{x}}_i]^T$, and

$$\begin{aligned}\hat{A}_i &= \hat{A}(\lambda_i) := \begin{bmatrix} 0 & 1 \\ -a(\lambda_i) & -b(\lambda_i) \end{bmatrix} \\ \hat{B}_i &= [0 \quad \sigma]^T, \quad \hat{C}_i = [1 \quad 0] \\ a(\lambda) &:= \alpha\lambda, \quad b(\lambda) := \theta + \gamma\alpha\lambda.\end{aligned}\tag{31c}$$

Even though functions $a(\lambda)$ and $b(\lambda)$ take different forms in continuous time, matrices \hat{A}_i , \hat{B}_i , and \hat{C}_i in (31c) have the same structure as their discrete-time counterparts in (14).

B. Optimal convergence rate

System (31) is stable if and only if the matrix \hat{A}_i is Hurwitz (i.e., if all of its eigenvalues have negative real parts). Moreover, the system is exponentially stable with the rate ρ ,

$$\|\hat{\psi}_i(\tau)\| \leq c e^{-\rho\tau} \|\hat{\psi}_i(0)\|$$

if and only if the real parts of all eigenvalues of \hat{A}_i are less than or equal to $-\rho$. For gradient flow dynamics (30a) with $\alpha = 1/L$, \hat{A}_i 's are real scalars and ρ is determined by

$$\rho_{\text{gfd}} := \min_i |\alpha\lambda_i| = m/L = 1/\kappa.\tag{32}$$

Note that \hat{A}_i in (31c) has the same structure as the matrix M in (16a). Lemma 8 is a continuous-time counterpart for Lemmas 1 and 2 and it provides conditions for (exponential) stability of matrices \hat{A}_i for accelerated gradient flow dynamics (30b).

Lemma 8: The real matrix M in (16a) satisfies

$$M \text{ is Hurwitz} \iff a, b > 0.$$

In addition, for any $\rho > 0$, we have

$$\max \{\Re(\text{eig}(M))\} \leq -\rho \iff \begin{cases} a \geq \rho(b - \rho) \\ b \geq 2\rho. \end{cases}$$

Proof: See Appendix F. ■

Conditions for stability and ρ -exponential stability in Lemma 8 respectively require inclusion of the point (b, a) to the open positive orthant and the ρ -parameterized cone shown in Figure 5. Furthermore, the normalization of the stepsize parameter to $\alpha = 1/L$ yields the extra condition $a \leq 1$. For $\rho < 1$, combining this inequality with the exponential stability conditions in Lemma 8 further restricts the ρ -exponential stability cone to the triangle in the (b, a) -plane,

$$\Delta_\rho := \{(b, a) \mid b \geq 2\rho, \rho(b - \rho) \leq a \leq 1\}\tag{33a}$$

whose vertices are given by

$$X_\rho = (2\rho, \rho^2), \quad Y_\rho = (2\rho, 1), \quad Z_\rho = (\rho + 1/\rho, 1).\tag{33b}$$

For $\rho = 1$, the triangle Δ_ρ is a single point and, for $\rho > 1$, adding the normalization condition $a \leq 1$ makes the ρ -exponential stability conditions in Lemma 8 infeasible. Thus, in what follows, we confine our attention to $\rho < 1$.

Figure 5 illustrates the stability and ρ -exponential stability cones as well as the ρ -exponential stability triangle Δ_ρ . Geometric properties of Δ_ρ allow us to determine the largest condition number for which (30b) is ρ -exponentially stable.

Proposition 4: For a strongly convex quadratic objective function $f \in \mathcal{Q}_m^L$ with the condition number $\kappa = L/m$, the optimal convergence rate and the corresponding parameters (β, γ) of accelerated gradient flow dynamics (30b) with $\alpha = 1/L$ are

$$\rho = 1/\sqrt{\kappa}, \quad \beta = 1 + (v - 2)/\sqrt{\kappa}, \quad \gamma = v\sqrt{\kappa}\tag{34}$$

where $v \in [0, 1]$. This rate is achieved by the heavy-ball method ($\gamma = 0$) with $v = 0$ and, for $\kappa \geq 4$, by Nesterov's accelerated method ($\gamma = \beta$) with $v = (\sqrt{\kappa} - 2)/(\kappa - 1)$.

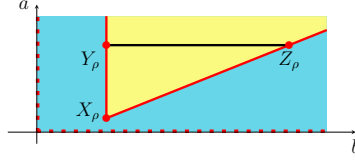


Figure 5. The open positive orthant (cyan) in the (b, a) -plane is the stability region for the matrix M in (16a). The intersections Y_ρ and Z_ρ of the stepsize normalization line $a = 1$ (black) and the boundary of the ρ -exponential stability cone (yellow) established in Lemma 8, along with the cone apex X_ρ determine the vertices of the ρ -exponential stability triangle Δ_ρ given by (33).

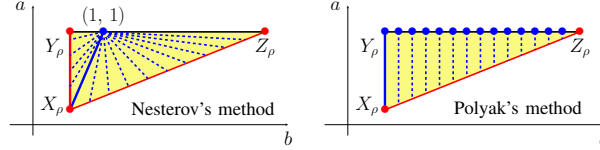


Figure 6. For a fixed ρ -exponential stability triangle Δ_ρ (yellow) in (33), the line segments $(b(\lambda), a(\lambda))$, $\lambda \in [m, L]$ for Nesterov's accelerated ($\gamma = \beta$) and the heavy-ball ($\gamma = 0$) dynamics, as special examples of accelerated dynamics (30b) with constant parameters γ, β , and $\alpha = 1/L$ are marked by dashed blue lines. The blue bullets correspond to the locus of the end point $(b(L), a(L))$, and the solid blue line segments correspond to the parameters for which the rate ρ is achieved for the largest possible condition number (34).

Proof: See Appendix F. ■

Proposition 4 uses necessary and sufficient condition for ρ -exponential stability: $(b(\lambda), a(\lambda)) \in \Delta_\rho$ for every $\lambda \in [m, L]$. Figure 6 illustrates the orientation of this line segment in Δ_ρ for the heavy-ball and Nesterov's algorithms. For the optimal values of parameters, Proposition 4 implies that accelerated gradient flow dynamics (30b) reduces settling time relative to gradient flow dynamics (30a) by a factor of $\sqrt{\kappa}$, i.e.,

$$\rho_{\text{agd}} / \rho_{\text{gfd}} = \sqrt{\kappa}.$$

C. Noise amplification

Similar to the discrete-time setting, exponentially stable LTI systems in (31) driven by white noise reach a statistical steady-state with $\lim_{t \rightarrow \infty} \mathbb{E}(\hat{\psi}_i(t)) = 0$. Furthermore, the variance

$$J := \lim_{t \rightarrow \infty} \frac{1}{t} \int_0^t \mathbb{E}(\|x(\tau) - x^*\|^2) d\tau \quad (35)$$

can be computed from the solution of the *continuous-time algebraic Lyapunov equation* [28]. The following theorem provides analytical expressions for the steady-state variance J .

Theorem 5: For a strongly convex quadratic objective function $f \in \mathcal{Q}_m^L$ with Hessian Q , the noise amplification J of (30) with any constant stabilizing parameters (α, β, γ) is determined by $J = \sum_{i=1}^n \hat{J}(\lambda_i)$. Here, $\hat{J}(\lambda_i)$ is the modal contribution of the i th eigenvalue λ_i of Q to the noise amplification

$$\hat{J}_{\text{gfd}}(\lambda) = \sigma^2 / (2a(\lambda)), \quad \hat{J}_{\text{agd}}(\lambda) = \sigma^2 / (2a(\lambda)b(\lambda))$$

where the functions a and b are given by (31c).

We omit the proof of Theorem 5 as it uses similar arguments to those used in the proof of [21, Theorem 1].

For $\alpha = 1/L$ and the parameters that optimize the convergence rate provided by Proposition 4, we can use the

explicit forms of $\hat{J}(\lambda)$ established in Theorem 5 to obtain

$$\begin{aligned} \frac{J_{\min}}{\sigma^2} &= \begin{cases} (\kappa + (n-1))/2 & \text{gfd} \\ (\kappa\sqrt{\kappa} + (n-1)\sqrt{\kappa})/4 & \text{agd (hb)} \\ (\kappa\sqrt{\kappa} + (n-1)2)/4 & \text{agd (na)} \end{cases} \\ \frac{J_{\max}}{\sigma^2} &= \begin{cases} ((n-1)\kappa + 1)/2 & \text{gfd} \\ ((n-1)\kappa\sqrt{\kappa} + \sqrt{\kappa})/4 & \text{agd (hb)} \\ ((n-1)\kappa\sqrt{\kappa} + 2)/4 & \text{agd (na)} \end{cases} \end{aligned} \quad (36)$$

For all three cases, the smallest noise amplification J_{\min} occurs when the Hessian matrix Q has $n-1$ eigenvalues at $\lambda = m$ and one at $\lambda = L$, and the largest noise amplification J_{\max} occurs when Q has $n-1$ eigenvalues at $\lambda = L$ and one at $\lambda = m$. Despite the $\sqrt{\kappa}$ improvement in the convergence rate achieved by the accelerated gradient flow dynamics, the corresponding J_{\min} and J_{\max} are larger than those of gradient flow dynamics by a factor of $\sqrt{\kappa}$. We next generalize this result to stabilizing (β, γ) and establish similar trends for all $f \in \mathcal{Q}_m^L$.

D. Convergence and noise amplification tradeoffs

The following result is the continuous-time analog of Theorem 2 and it establishes a lower bound on the product of the noise amplification and the settling time $1/\rho$ of the accelerated gradient flow dynamics for any choice of (β, γ) .

Theorem 6: Let the parameters (β, γ) be such that the accelerated gradient flow dynamics (30b) with $\alpha = 1/L$ is ρ -exponentially stable for all $f \in \mathcal{Q}_m^L$. Then, J_{\min} and J_{\max} in (9) satisfy,

$$\frac{J_{\min}}{\rho} \geq \frac{\sigma^2 \kappa^2}{4} + \frac{(n-1)\sigma^2}{2(1+\rho^2)} \quad (37a)$$

$$\frac{J_{\max}}{\rho} \geq (n-1) \frac{\sigma^2 \kappa^2}{4} + \frac{\sigma^2}{2(1+\rho^2)}. \quad (37b)$$

Proof: See Appendix F. ■

Theorem 6 demonstrates that the tradeoff between J_{\min} and J_{\max} and the settling time established in Theorem 2 for the two-step momentum algorithm extends to continuous-time dynamics. For a fixed problem size n and the parameters that optimize the convergence rate provided in Lemma 8, we can use (36) to conclude that the bounds in Theorem 6 are order-wise tight.

VII. PROOFS OF THEOREMS 1 AND 2

A. Proof of Theorem 1

From Theorem 4 it follows that we can use upper bounds on $\hat{J}(\lambda)$ over $\lambda \in [m, L]$ to establish an upper bound on J . Since the algorithm achieves the convergence rate ρ , combining equation (15) and Lemma 2 yield $(b(\lambda), a(\lambda)) \in \Delta_\rho$ for all $\lambda \in [m, L]$. As we demonstrate in Appendix B, the function \hat{J} is convex in (b, a) over the stability triangle Δ . In addition, $\Delta_\rho \subset \Delta$ is the convex hull of the points X_ρ, Y_ρ, Z_ρ in the (b, a) -plane. Since the maximum of a convex function over the convex hull of a finite set of points is attained at one of these points, \hat{J} attains its maximum over Δ_ρ at X_ρ, Y_ρ , or Z_ρ .

Using the definition of X_ρ, Y_ρ , and Z_ρ in (18c), the affine relations (23), and the analytical expression for \hat{J} in Theorem 4, it follows that the maximum occurs at the vertices X_ρ and Y_ρ ,

$$\hat{J}_{\max} = \frac{\sigma^2(1+\rho^2)}{(1-\rho)^3(1+\rho)^3}$$

where we use $d_{X_\rho} = l_{Y_\rho} = (1-\rho)^2$, $l_{X_\rho} = d_{Y_\rho} = (1+\rho)^2$, and $h_{X_\rho} = h_{Y_\rho} = 1-\rho^2$. Combining the above identity with Theorem 4 completes the proof of (11a).

To prove (11b), we use an argument similar to the proof of Proposition 1. For $d(L)$ associated with the point $(b(L), a(L))$,

$$\alpha L = d(L) \leq d_{\max} = (1+\rho)^2$$

where d_{\max} is the largest value that d can take among all points $(b, a) \in \Delta_\rho$; see equation (20a). Combining this inequality with $\sigma = \alpha\sigma_a$ and (11a) completes the proof of Theorem 1.

B. Proof of Theorem 2

Using the expression $J = \sum_i \hat{J}(\lambda_i)$ established in Theorem 4, we have the decomposition

$$\frac{J}{1-\rho} = \frac{\hat{J}(m) + \sum_{i=1}^{n-1} \hat{J}(\lambda_i)}{1-\rho}. \quad (38)$$

To lower bound the quantity $J_{\min}/(1-\rho)$, we establish a lower bound on $\hat{J}(m)/(1-\rho)$ that scales quadratically with κ , and also a general lower bound on $\hat{J}(\lambda)/(1-\rho)$, which we use to bound the other terms in the summation.

Case $\sigma = \sigma_a$: The proof relies on the inequalities

$$\frac{\hat{J}(m)}{1-\rho} \geq \frac{\sigma^2 \kappa^2}{2(1+\rho)^5} \quad (39a)$$

$$\frac{\hat{J}(\lambda)}{1-\rho} \geq \frac{\sigma^2(\sqrt{\kappa} + 1)}{2}. \quad (39b)$$

We first prove (39a). Our approach builds on the proof of Proposition 1. In particular, we let $d(\lambda) = \alpha\lambda$ be the d -value associated with the point $(b(\lambda), a(\lambda))$, where d and (b, a) are defined in (23) and (14c), respectively. We thus have

$$d(m) = d(L)/\kappa.$$

In addition, by Lemma 3, $(b(\lambda), a(\lambda)) \in \Delta_\rho$ for $\lambda \in [m, L]$. Thus, using the trivial inequality $d(L) \leq d_{\max}$, we obtain that

$$d(m) \leq d_{\max}/\kappa = (1+\rho)^2/\kappa \quad (40)$$

where $d_{\max} = (1+\rho)^2$ is the largest value that d can take among all points $(b, a) \in \Delta_\rho$; see equation (20a). We now use Theorem 4 to write

$$\frac{\hat{J}(\lambda)}{1-\rho} = \frac{\sigma^2(d(\lambda) + l(\lambda))}{2d(\lambda)h(\lambda)l(\lambda)(1-\rho)} \geq \frac{\sigma^2}{2d(\lambda)h(\lambda)(1-\rho)}. \quad (41)$$

To lower bound the right-hand side of (41), we invoke a simple geometric argument as follows. Let \mathcal{L} be the line that passes through $(b(\lambda), a(\lambda))$ and is parallel to the edge XZ of the stability triangle Δ , and let G be the intersection of \mathcal{L} and the edge $X_\rho Z_\rho$ of the ρ -stability triangle Δ_ρ , as illustrated in Figure 7. It is easy to verify that

$$h_G \geq h(\lambda), \quad d_G = d(\lambda) \quad (42a)$$

where h_G and d_G correspond to the h and d values associated with the point G . In addition, since G lies on the edge $X_\rho Z_\rho$, h_G and d_G satisfy the affine relation

$$h_G = 1 - \rho + \rho/(1 - \rho) d_G. \quad (42b)$$

This can be obtained by computing the equation of the line $X_\rho Z_\rho$ in the $b - a$ plane and using the definitions of d and h in (23). We can now write

$$\frac{\sigma^2}{2d(\lambda)h(\lambda)(1-\rho)} \stackrel{(a)}{\geq} \frac{\sigma^2}{2d(\lambda)h_G(1-\rho)} \stackrel{(b)}{=} \frac{\sigma^2}{2d(\lambda)((1-\rho)^2 + \rho d(\lambda))} \quad (43a)$$

where (a) and (b) follow from (42a) and (42), respectively. For $\lambda = m$, we can further write

$$\frac{\sigma^2}{2d(m)((1-\rho)^2 + \rho d(m))} \geq \frac{\sigma^2}{2 \frac{(1+\rho)^2}{\kappa} \left(\frac{(1+\rho)^2}{\kappa} + \rho \frac{(1+\rho)^2}{\kappa} \right)} = \frac{\sigma^2 \kappa^2}{2(1+\rho)^5} \quad (43b)$$

where the inequality is obtained by combining (21) and (40). Combining (41) and (43) completes the proof of (39a).

Next, we prove the general lower bound in (39b). As we demonstrate in Appendix B, the modal contribution \hat{J} to the noise amplification is a convex function of (b, a) and it takes its minimum $\hat{J}_{\min} = \sigma^2$ over the stability triangle Δ at the origin $b = a = 0$. Combining this fact with the lower bound in (6) on ρ completes the proof of (39b).

Finally, we can obtain the desired lower bound on the quantity $J_{\min}/(1-\rho)$ by combining (38) and (39).

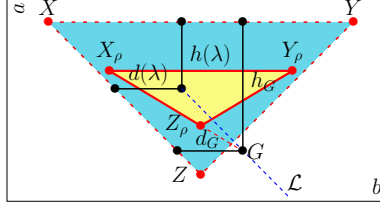


Figure 7. The line \mathcal{L} (blue, dashed) and the intersection point G , along with the distances d_1 , h_1 , d_G , and h_G as introduced in the proof of Theorem 2.

Case $\sigma = \alpha\sigma_a$: The proof relies on the inequalities

$$\frac{\hat{J}(\lambda)}{1-\rho} \geq \frac{\sigma_a^2}{2\lambda^2(1+\rho)} \quad (44a)$$

$$\frac{\hat{J}(\lambda)}{1-\rho} \geq \frac{\sigma_a^2(1-\rho)^3\kappa^2}{L^2}. \quad (44b)$$

For $\lambda = m$, we use (44a), and for general λ , we take the maximum of (44a) and (44b).

We first prove (44a). We combine (41) and (43a) to obtain

$$\frac{\hat{J}(\lambda)}{1-\rho} \geq \frac{\alpha^2\sigma_a^2}{2d(\lambda)((1-\rho)^2 + \rho d(\lambda))}. \quad (45)$$

Noting that

$$d(\lambda) \geq d_{\min} := (1-\rho)^2 \quad (46)$$

where d_{\min} is the smallest value that d can take among all points $(b, a) \in \Delta_\rho$, [cf. (20b)], we can write

$$\frac{\alpha^2\sigma_a^2}{2d(\lambda)((1-\rho)^2 + \rho d(\lambda))} \geq \frac{\alpha^2\sigma_a^2}{2d(\lambda)^2(1+\rho)} = \frac{\sigma_a^2}{2\lambda^2(1+\rho)}. \quad (47)$$

Combining (45) and (47) completes the proof of (44a).

To prove (44b) we can simply use the inequality in (46) and $d(m) = \alpha m$, to obtain $\alpha \geq (1-\rho)^2\kappa/L$. Combining this inequality with $\hat{J}_{\min} = \sigma^2 = \alpha^2\sigma_a^2$ yields (44b).

Finally, we can obtain the desired lower bound on the quantity $J_{\min}/(1-\rho)$ by combining (38) and (44).

To obtain the desired lower bounds on $J_{\max}/(1-\rho)$, we consider a function for which the Hessian has $n-1$ eigenvalues at $\lambda = m$ and one eigenvalue at $\lambda = L$. For such a function, we can use Theorem 4 to write

$$\frac{J_{\max}}{1-\rho} \geq \frac{J}{1-\rho} = \frac{(n-1)\hat{J}(m) + \hat{J}(L)}{1-\rho}. \quad (48)$$

Case $\sigma = \sigma_a$: We use the inequalities in (39a) and (39b) to bound $\hat{J}(m)/(1-\rho)$ and $\hat{J}(L)/(1-\rho)$ in (48), respectively.

Case $\sigma = \alpha\sigma_a$: We use the inequality in (44a) with $\lambda = m$ to lower bound $\hat{J}(m)/(1-\rho)$, and combine (44a) and (44b) to lower bound $\hat{J}(L)/(1-\rho)$ in (48). This completes the proof.

VIII. CONCLUDING REMARKS

We study a class of two-step momentum algorithms in which the iterates are perturbed by an additive white noise. For this class of problems, we establish lower bounds on the product of the settling time and the smallest/largest steady-state variance of the error in the optimization variable. These bounds scales as κ^2 for all stabilizing parameters and they reveal a fundamental limitation imposed by the condition number in designing algorithms that tradeoff noise amplification and convergence rate. In addition, we provide a novel geometric viewpoint that brings insight into the relation between noise amplification, convergence rate, and algorithmic parameters. Our viewpoint (i) provides an alternative approach to finding parameters that yield optimal convergence rates for the heavy-ball and Nesterov's accelerated methods; and (ii) allows us to introduce two parameterized families of accelerated algorithms for which the parameters can be adjusted to tradeoff noise amplification and settling time while preserving order-wise Pareto optimality. We also extend our analysis to continuous-time dynamical systems that can be discretized via an implicit-explicit Euler scheme to obtain the two-step momentum algorithm. For such gradient flow dynamics, we uncover similar fundamental stochastic performance limitations as in discrete time. Our ongoing work includes extending these results to first-order algorithms with more complex structures including update strategies that involve information from more than the last two iterates.

ACKNOWLEDGMENTS

We thank Laurent Lessard for his comments on an earlier draft of this manuscript.

APPENDIX

A. Settling time

If ρ denotes the linear convergence rate, $1/(1 - \rho)$ quantifies the *settling time*. For any desired accuracy $\|\psi^t\|/\|\psi^0\| \leq \epsilon$, (5) can be used to obtain $c\rho^t \leq \epsilon$. Taking the logarithm and using the first-order Taylor series approximation $\log(1 - x) \approx -x$ around $x = 0$ yields

$$t \geq \log(\epsilon/c)/\log(\rho) \approx \log(c/\epsilon)/(1 - \rho).$$

In continuous time, the sufficient condition for reaching ϵ -accuracy $ce^{-\rho t} \leq \epsilon$ yields $t \geq \log(c/\epsilon)/\rho$, and $1/\rho$ can be used to asses the settling time.

B. Convexity of modal contribution \hat{J} to noise amplification

To show the convexity of \hat{J} , we use the fact that the function $g(x) = \prod_{i=1}^d x_i^{-1}$ is convex over the positive orthant \mathbb{R}_{++}^d . This can be verified by noting that its Hessian satisfies

$$\nabla^2 g(x) = g(x) (\text{diag}(x) + xx^T) \succ 0$$

where $\text{diag}(\cdot)$ is the diagonal matrix. By Theorem 4, we have

$$\frac{\hat{J}}{\sigma^2} = \frac{d + l}{2dh} = \frac{1}{2hd} + \frac{1}{2hl}$$

where we have dropped the dependence on λ for simplicity. The functions $1/(2hd)$ and $1/(2hl)$ are both convex over the positive orthant $d, h, l > 0$. Thus, \hat{J} is convex with respect to (d, h, l) . In addition, since d, h , and l are all affine functions of a and b , we can use the equivalence relation in (24a) to conclude that \hat{J} is also convex in (b, a) over the stability triangle Δ . Finally, since $b(\lambda)$ and $a(\lambda)$ are affine in λ , it follows that for any stabilizing parameters, \hat{J} is also convex with respect to λ over the interval $[m, L]$.

Convexity of \hat{J} allows us to use first-order conditions to find its minimizer. In particular, using the partial derivatives

$$\begin{aligned} \frac{\partial \hat{J}}{\partial d} &= -\frac{1}{2hd^2}, & \frac{\partial \hat{J}}{\partial l} &= -\frac{1}{2hl^2}, & \frac{\partial \hat{J}}{\partial h} &= -\frac{l + d}{2h^2dl} \\ \frac{\partial d}{\partial a} &= \frac{\partial l}{\partial a} = -\frac{\partial h}{\partial a} = \frac{\partial d}{\partial b} = -\frac{\partial l}{\partial b} = 1, & \frac{\partial h}{\partial b} &= 0 \end{aligned}$$

it is easy to verify that $\partial \hat{J}/\partial a = \partial \hat{J}/\partial b = 0$ at $a = b = 0$. Thus, \hat{J} takes its minimum $\hat{J}_{\min} = \sigma^2$ over the stability triangle Δ at $b = a = 0$, which corresponds to $d = h = l = 1$.

C. Proofs of Section IV

1) *Proof of Lemma 1:* The equivalence between $(b, a) \in \Delta$ and $\rho(M) < 1$ is a direct consequence of the Jury stability criterion [29, Chap. 4-3]. The characteristic polynomial $F(z)$ associated with the matrix M in (16a) is given by (16b) and the necessary and sufficient conditions for stability are

$$|a| < 1, \quad F(\pm 1) = 1 \pm b + a > 0.$$

The condition $a > -1$ is ensured by the positivity of $F(\pm 1)$ and can be omitted. This completes the proof.

2) *Proof of Lemma 2:* We start by noting that $\rho(M) \leq \rho$ if and only if $\rho(M') \leq 1$ where $M' = M/\rho$. The characteristic polynomial for M' , $z^2 + (b/\rho)z + a/\rho^2$, allows us to use similar arguments to those presented in the proof of Lemma 1 to show that

$$\rho(M') \leq 1 \iff (b/\rho, a/\rho^2) \in \Delta_1 \quad (49)$$

where $\Delta_1 := \{(b, a) \mid |b| - 1 \leq a \leq 1\}$ is the closure of the set Δ in (17b). Finally, it is easy to show that the condition on the right-hand side of (49) is equivalent to $(b, a) \in \Delta_\rho$, where Δ_ρ is given by (18b). This completes the proof.

Remark 4: The eigenvalues of the matrix M in (16a) are determined by $(-b \pm \sqrt{b^2 - 4a})/2$, and the sign of $b^2 - 4a$ determines if the eigenvalues are real or complex. The condition $b^2 = 4a$ corresponds to a parabola that passes through the vertices $X_\rho = (-2\rho, \rho^2)$ and $Y_\rho = (2\rho, \rho^2)$ of the triangle Δ_ρ and it is adjacent to the edges $X_\rho Z_\rho$ and $Y_\rho Z_\rho$ for all $\rho < 1$; see Figure 8. For the optimal values of parameters provided in Table I, we can combine this observation and the information in Figure 3 to conclude that, in contrast to gradient descent where the eigenvalues of the matrix A in (4a) are all real, for Nesterov's method the eigenvalues can be both real and complex, whereas the heavy-ball algorithm only involves complex conjugate pairs of eigenvalues.

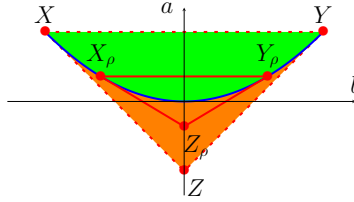


Figure 8. The green and orange subsets of the stability triangle Δ (dashed-red) correspond to complex conjugate and real eigenvalues for the matrix M in (16a), respectively. The blue parabola $b^2 = 4a$ corresponds to M with repeated eigenvalues and it is tangent to the edges $X_\rho Z_\rho$ and $Y_\rho Z_\rho$ of the ρ -linear convergence triangle Δ_ρ (solid red).

3) *Proof of Equation (22c):* According to Figure 3, in order to find the largest ratio $d(L)/d(m)$ over the ρ -linear convergence set Δ_ρ for Nesterov's accelerated method, we need to check the pairs of points $\{E, E'\}$ that lie on the boundary of the triangle Δ_ρ , whose line segment EE' passes through the origin O . If one of the end points E lies on the edge $X_\rho Y_\rho$, then depending on whether the other end point E' lies on the edge $X_\rho Z_\rho$ or $Y_\rho Z_\rho$, we can continuously increase the ratio $d_E/d_{E'}$ by moving E toward the vertices Y_ρ or X_ρ , respectively. Thus, this case reduces to checking only the ratio $d_E/d_{E'}$ for the line segments $X_\rho X'_\rho$ and $Y_\rho Y'_\rho$, where

$$X'_\rho = (2\rho/3, -\rho^2/3), \quad Y'_\rho = (-2\rho/3, -\rho^2/3) \quad (50)$$

are the intersections of OX_ρ with $Y_\rho Z_\rho$, and OY_ρ with $X_\rho Z_\rho$; see Figure 9. Regarding the case where neither E nor E' lies on the edge $X_\rho Y_\rho$, let us assume without loss of generality that E and E' lie on $Y_\rho Z_\rho$ and $X_\rho Z_\rho$, respectively. In this case, it is straightforward to parameterize the ratio by

$$\frac{d_E}{d_{E'}} = \frac{(1+c)(1/(1-\rho)-c)}{(1-c)(1/(1+\rho)+c)}, \quad c \in [-1/2, 1/2] \quad (51)$$

where $c\rho$ determines the slope of EE' . The general shape of this function is provided in Figure 10. It is easy to verify that $d_E/d_{E'}$ takes its maximum over $c \in [-1/2, 1/2]$ at one of the boundaries. Thus, this case also reduces

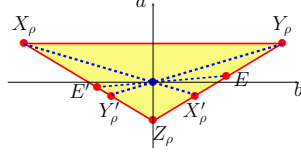


Figure 9. The points X'_ρ and Y'_ρ as defined in (50) along with an arbitrary line segment EE' passing through the origin.

to checking only the ratio $d_E/d_{E'}$ for the line segments $X_\rho X'_\rho$ and $Y_\rho Y'_\rho$. We complete the proof by noting that

$$\frac{d_{X'_\rho}}{d_{X_\rho}} = \frac{(1+\rho)(3-\rho)}{3(1-\rho)^2}, \quad \frac{d_{Y_\rho}}{d_{Y'_\rho}} = \frac{3(1+\rho)^2}{(3+\rho)(1-\rho)}$$

which satisfy $d_{X'_\rho}/d_{X_\rho} > d_{Y_\rho}/d_{Y'_\rho}$.

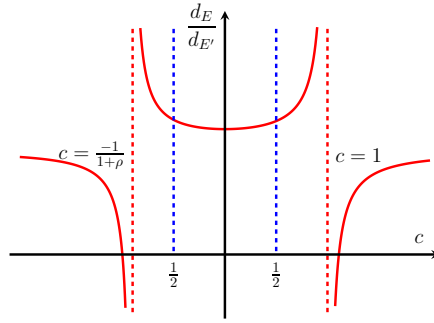


Figure 10. The ratio $d_E/d_{E'}$ in (51) for Nesterov's method, where E and E' lie on the edges $Y_\rho Z_\rho$ and $X_\rho Z_\rho$ of the ρ -linear convergence triangle Δ_ρ , and $c\rho$ determines the slope of EE' which passes through the origin.

D. Proofs of Section V

1) *Proof of Lemma 4:* We show that the parameters α, β, γ correspond to the family of heavy-ball type methods in which the end points of the line segment $(b(\lambda), a(\lambda))$, $\lambda \in [m, L]$ lie on the edges $X_\rho Z_\rho$ and $Y_\rho Z_\rho$ of the ρ -linear convergence triangle Δ_ρ . In particular, we can use a scalar $c \in [0, 1]$ to parameterize the end points as

$$\begin{aligned} (b(m), a(m)) &= (-(1+c)\rho, c\rho^2) \\ (b(L), a(L)) &= ((1+c)\rho, c\rho^2). \end{aligned}$$

Using the definition of a, b in (14c), we can solve the above equations for α, β , and γ to verify the desired parameters. Thus, the algorithm achieves the convergence rate ρ . In this case, the extreme points $c = 0$ and $c = 1$ recover gradient descent and the heavy-ball method with the parameters that yield the optimal settling times; see Table I.

Furthermore, h, d , and l in (23) are given by

$$\begin{aligned} h(m) &= h(L) = 1 - c\rho^2 \\ d(m) &= l(L) = (1-\rho)(1-c\rho) \\ l(m) &= d(L) = (1+\rho)(1+c\rho) \end{aligned} \tag{52a}$$

and the condition number is determined by

$$\kappa = \frac{\alpha L}{\alpha m} = \frac{d(L)}{d(m)} = \frac{l(m)}{d(m)}. \tag{52b}$$

By combining this identity with the expressions in (52a), and rearranging terms, we can obtain the desired expression for c in terms of ρ and κ .

Using the analytical expressions in Theorem 4, it follows that $\hat{J}(\lambda)$ is symmetric over $[m, L]$, i.e., $\hat{J}(\lambda) = \hat{J}(m + L - \lambda)$ for all $\lambda \in [m, L]$. In addition, as we demonstrate in Appendix B, $\hat{J}(\lambda)$ is convex. Therefore, $\hat{J}(\lambda)$ attains its maximum at the boundaries $\lambda = m$ and $\lambda = L$. To obtain the maximum value, we use the expression for $\hat{J}(\lambda)$ in Theorem 4 to write

$$\hat{J}(m) = \frac{d(m) + l(m)}{2h(m)d(m)l(m)} = \frac{\kappa + 1}{2h(m)l(m)} \quad (52c)$$

where the second equality follows from (52b). Combining (52a) and (52c) yields the expression for $\hat{J}(m)$.

Also, from symmetry and convexity, it follows that $\hat{J}(\lambda)$ attains its minimum at the midpoint $\lambda = \hat{\lambda} := (m + L)/2 = (1 + \beta)/\alpha$. Note that this point corresponds to $(b(\hat{\lambda}), a(\hat{\lambda})) = (0, c\rho^2)$ in the (b, a) -plane and thus it satisfies

$$h(\hat{\lambda}) = 1 - c\rho^2, \quad d(\hat{\lambda}) = l(\hat{\lambda}) = 1 + c\rho^2. \quad (52d)$$

Evaluating the expression for $\hat{J}(\lambda)$ at the point $\lambda = \hat{\lambda}$ using (52d) yields the desired minimum value.

2) *Proof of Lemma 5:* To bound the largest quantity $\hat{J}_{\max}/(1 - \rho) = \hat{J}(m)/(1 - \rho)$, we use (52b) and (52c) to write $\hat{J}(m) = \kappa(\kappa + 1)/(2h(m)l(m)^2/d(m))$. Combining this identity with the trivial inequalities

$$1 \leq (1 - \rho)h(m)/d(m) \leq 1 + c\rho$$

we obtain that

$$\frac{\kappa(\kappa + 1)}{2(1 + c\rho)l(m)^2} \leq \frac{\hat{J}(m)}{1 - \rho} \leq \frac{\kappa(\kappa + 1)}{2l(m)^2}.$$

This completes the proof of the bounds on $\hat{J}(m)/(1 - \rho)$.

For bounding $\hat{J}_{\min}/(1 - \rho) = \hat{J}(\hat{\lambda})/(1 - \rho)$, we can write

$$\begin{aligned} \hat{J}(\hat{\lambda}) &= \frac{\sigma^2}{(1 - c\rho^2)(1 + c\rho^2)} \leq \frac{\sigma^2}{(1 - c\rho)(1 + c\rho^2)} \\ &= \frac{\sigma^2 \kappa(1 - \rho)}{(1 + \rho)(1 + c\rho)(1 + c\rho^2)} \leq \frac{\sigma^2 \kappa(1 - \rho)}{(1 + \rho)(1 + c\rho^2)^2} \end{aligned}$$

where the last equality follows from (52a) and (52b). Also,

$$\begin{aligned} \hat{J}(\hat{\lambda}) &= \frac{\sigma^2}{(1 - c\rho^2)(1 + c\rho^2)} \geq \frac{\sigma^2}{(1 - c^2\rho^2)(1 + c\rho^2)} \\ &= \frac{\sigma^2 \kappa(1 - \rho)}{(1 + \rho)(1 + c\rho)^2(1 + c\rho^2)} \geq \frac{\sigma^2 \kappa(1 - \rho)}{(1 + \rho)(1 + c\rho)^3} \end{aligned}$$

where the last equality follows from (52a) and (52b). Finally, the bounds on θ_i s defined in (26) follow from $c, \rho \in [0, 1]$.

3) *Proof of Lemma 6:* We show that the parameters α, β, γ correspond to the family of Nesterov type methods in which the end points of the line segment $(b(\lambda), a(\lambda))$, $\lambda \in [m, L]$ lie on the edges $X_\rho Z_\rho$ and $Y_\rho Z_\rho$ of the ρ -linear convergence triangle Δ_ρ . In particular, we can use a scalar $c \in [0, 1/2]$ to parameterize the lines passing through the origin via $a = -c\rho b$. This yields

$$\begin{aligned} (b(m), a(m)) &= (-\rho/(1 - c), c\rho^2/(1 - c)) \\ (b(L), a(L)) &= (\rho/(1 + c), -c\rho^2/(1 + c)). \end{aligned}$$

Using the definition of a, b in (14c), we can solve the above equations for α, β, γ to verify the desired parameters. Thus, the algorithm achieves the convergence rate ρ . In this case, the extreme points $c = 0$ and $c = 1/2$ recover gradient descent and Nesterov's method with the algorithm parameters that yield the optimal settling times $1/(1 - \rho) = (\kappa + 1)/1$ and $1/(1 - \rho) = (\sqrt{3\kappa + 1})/2$ provided by Table I, respectively.

Furthermore, the values of h , d , l in (23) are given by

$$\begin{aligned}
h(m) &= (1 - c - c\rho^2)/(1 - c) \\
d(m) &= (1 - \rho)(1 - c - c\rho)/(1 - c) \\
l(m) &= (1 + \rho)(1 - c + c\rho)/(1 - c) \\
h(L) &= (1 + c + c\rho^2)/(1 + c) \\
d(L) &= (1 + \rho)(1 + c - c\rho)/(1 + c) \\
l(L) &= (1 - \rho)(1 + c + c\rho)/(1 + c)
\end{aligned} \tag{53a}$$

and the condition number is determined by

$$\kappa = \frac{\alpha L}{\alpha m} = \frac{d(L)}{d(m)} = \frac{l(m)}{r d(m)} \tag{53b}$$

where we let $r := l(m)/d(L)$. By combining this identity with the expressions in (53a), and rearranging terms, we can obtain the desired quadratic equation for c in terms of ρ and κ . To see $r \in [1, 3]$, observe in Figure 3 that as we continuously vary the orientation from gradient descent ($c = 0$) to Nesterov's method with parameters that yield optimal convergence rate ($c = 1/2$), the values $l(m)$ and $1/d(L)$ continuously increase. Thus, r is also increasing in c , and its smallest and largest values can be obtained for $c = 0$ and $c = 1/2$, respectively. This yields $1 \leq r \leq 3(1 + \rho)/(3 - \rho) \leq 3$.

As we demonstrate in Appendix B, \hat{J} as a function of (b, a) takes its minimum $\hat{J}_{\min} = \sigma^2$ at the origin. In addition, for each $c \in [0, 1/2]$, the line segment $(b(\lambda), a(\lambda))$, $\lambda \in [m, L]$ passes through the origin at $\lambda = 1/\alpha$. Thus, the minimum of $\hat{J}(\lambda)$ occurs at $\lambda = 1/\alpha$ and is given by $\hat{J}_{\min} = \sigma^2$.

We next show that $\hat{J}(m)$ is the maximum value that $\hat{J}(\lambda)$ takes over $[m, L]$. Note that $\hat{J}(\lambda)$ is a convex function of λ ; see Appendix B. Therefore, it attains its maximum at one of the boundary points $\lambda = m$ and $\lambda = L$. To show $\hat{J}(m) > \hat{J}(L)$, we first compute the formula for $\hat{J}(m)$ and $\hat{J}(L)$ in terms of ρ and c by combining (53a) and the analytical expression for \hat{J} in Theorem 4. By properly rearranging terms and simplifying fractions, we can obtain the equivalence

$$\hat{J}(m) \geq \hat{J}(L) \iff c^4 \rho^4 - c^4 \rho^2 - c^2 \rho^2 - c^2 + 1 \geq 0.$$

For $\rho \in [0, 1]$ and $c \in [0, 1/2]$, it is easy to verify that the inequality on the right-hand holds as desired.

To obtain the maximum value, we use Theorem 4 to write

$$\hat{J}(m) = \frac{d(m) + l(m)}{2h(m)d(m)l(m)} = \frac{r\kappa + 1}{2h(m)l(m)}. \tag{53c}$$

Combining (53a) with (53c) yields the desired value for $\hat{J}(m)$.

E. Proof of Lemma 7

To obtain the desired upper and lower bounds on $\hat{J}_{\max}/(1 - \rho) = \hat{J}(m)/(1 - \rho)$, we combine (53b) and (53c) to write

$$\hat{J}(m) = \frac{r\kappa(r\kappa + 1)}{2h(m)(l(m))^2/d(m)}.$$

This equation in conjunction with the trivial inequalities

$$1 \leq (1 - \rho)h(m)/d(m) \leq 1 + \rho$$

allows us to write

$$\frac{r\kappa(r\kappa + 1)}{2(1 + \rho)(l(m))^2} \leq \frac{\hat{J}(m)}{1 - \rho} \leq \frac{r\kappa(r\kappa + 1)}{2(l(m))^2}. \tag{53d}$$

Combining (53a) and (53d) yields the desired bounds on $\hat{J}_{\max}/(1 - \rho)$. Finally, the bounds on $\hat{J}_{\min}/(1 - \rho) = \sigma^2/(1 - \rho)$ can be obtained by noting that $1/(1 - \rho) \in [\sqrt{3\kappa + 1}/2, (\kappa + 1)/2]$ as shown in Lemma 6.

F. Proofs of Section VI

1) *Proof of Lemma 8:* The condition for stability can be verified using the Routh-Hurwitz criterion applied to the characteristic polynomial associated with the matrix M . Similarly, the condition for ρ -exponential stability can be obtained by applying the Routh-Hurwitz criterion to the characteristic polynomial associated with the matrix $M + \rho I$, i.e.,

$$s^2 + (b - 2\rho)s + \rho^2 - \rho b + a = 0$$

and noting that strict inequalities become non-strict as we require $\Re(\text{eig}(M - \rho I))$ to be non-positive. This completes the proof.

2) *Proof of Proposition 4:* The ρ -exponential stability of (30b) with $\alpha = 1/L$ is equivalent to the inclusion of the line segment $(b(\lambda), a(\lambda))$, $\lambda \in [m, L]$ in the triangle Δ_ρ in (33), where $a(\lambda)$, $b(\lambda)$ are given by (31c). In addition, using the convexity of Δ_ρ , this condition further reduces to the end points

$$(b(L), a(L)), (b(m), a(m)) \in \Delta_\rho.$$

Now since $a(L) = 1$, $a(m) = 1/\kappa$, the above condition implies

$$a_{\max}/a_{\min} \geq \kappa \quad (54)$$

where a_{\max} and a_{\min} are the largest and smallest values that a can take among all $(b, a) \in \Delta_\rho$. It is now easy to verify that $a_{\max} = 1$ and $a_{\min} = \rho^2$, and they correspond to the edge $Y_\rho Z_\rho$ and the vertex X_ρ of Δ_ρ , respectively; see Figure 5. Thus, inequality (54) yields the upper bound $\rho \leq 1/\sqrt{\kappa}$. Furthermore, to achieve this rate, we can let

$$(b(m), a(m)) = X_\rho, \quad (b(L), a(L)) = E_v \quad (55)$$

where $E_v := (b_v, 1) = (2\rho + v(\rho - 1/\rho), 1)$, $v \in [0, 1]$ parameterizes the edge $Y_\rho Z_\rho$. Solving the equations in (55) for γ and β yields the optimal parameter values. Finally, letting $\gamma = 0$ and $\gamma = \beta$ yield the conditions on v for the heavy-ball and Nesterov's method, respectively. The condition $\kappa \geq 4$ for Nesterov's method stems from the fact that, for $\alpha = 1/L$, setting $\gamma = \beta$ yields $b(L) = 1$. Thus, we have the necessary condition $2\rho \leq 1$ to ensure $(b(L), a(L)) \in \Delta_\rho$; see Figure 6. This completes the proof.

3) *Proof of Theorem 6:* Let $G := (b_G, a_G)$ be the point on the edge $X_\rho Z_\rho$ of the triangle Δ_ρ in (33) such that

$$a_G = a(m), \quad b_G = a(m)/\rho + \rho.$$

Using $(b(m), a(m)) \in \Delta_\rho$, it is easy to verify that $b_G \geq b(m)$. This allows us to write

$$\begin{aligned} \frac{\hat{J}(m)}{\rho} &= \frac{\sigma^2}{2a(m)b(m)\rho} \\ &\geq \frac{\sigma^2}{2a(m)b_G\rho} = \frac{\sigma^2}{2a(m)(a(m) + \rho^2)}. \end{aligned}$$

Combining the above inequality with $a(m) = 1/\kappa$ and the upper bound $\rho \leq 1/\sqrt{\kappa}$ from Lemma 8 yields

$$\hat{J}(m)/\rho \geq \sigma^2 \kappa^2 / 4. \quad (56)$$

Noting that among the points in Δ_ρ , the modal contribution function $\hat{J} = \sigma^2/(2ab)$ takes its minimum value

$$\hat{J}_{\min} = \sigma^2/(2\rho + 2/\rho) \quad (57)$$

at the vertex $Z_\rho = (1, \rho + 1/\rho)$, we can write

$$\frac{J}{\rho} = \frac{\hat{J}(m)}{\rho} + \sum_{i=1}^{n-1} \frac{\hat{J}(\lambda_i)}{\rho} \geq \frac{\sigma^2 \kappa^2}{4} + \frac{(n-1)\sigma^2}{2(1 + \rho^2)}$$

where we used (56) to lower bound the first term $\hat{J}(m)/\rho$. This completes the proof of (37a).

To prove the lower bound in (37b), we consider a function for which the Hessian has $n-1$ eigenvalues at $\lambda = m$

and one eigenvalue at $\lambda = L$. For such a function, we can write

$$J_{\max} \geq J = \hat{J}(m)(n-1) + \hat{J}(L).$$

Finally, we lower bound the right hand-side using (56) and (57) to complete the proof.

G. Lyapunov equations and steady-state variance

For the discrete-time LTI system in (4a), the covariance matrix $P^t := \mathbb{E}(\psi^t(\psi^t)^T)$ of the state vector ψ^t satisfies the linear recursion

$$P^{t+1} = AP^tA^T + BB^T \quad (58a)$$

and its steady-state limit

$$P := \lim_{t \rightarrow \infty} \mathbb{E}(\psi^t(\psi^t)^T) \quad (58b)$$

is the unique solution to the algebraic Lyapunov equation [28],

$$P = APA^T + BB^T. \quad (58c)$$

For stable LTI systems, performance measure (7) can be computed using

$$J = \lim_{t \rightarrow \infty} \frac{1}{t} \sum_{k=0}^t \text{trace}(Z^k) = \text{trace}(Z) \quad (58d)$$

where $Z = CPC^T$ is the steady-state limit of the output covariance matrix $Z^t := \mathbb{E}(z^t(z^t)^T) = CP^tC^T$. We can prove Theorem 4 by finding the solution P to (58c) for the two-step momentum algorithm.

The above results carry over to the continuous-time case with the only difference that the Lyapunov equation for the steady-state covariance matrix is given by

$$0 = AP + PA^T + BB^T.$$

REFERENCES

- [1] B. T. Polyak, "Some methods of speeding up the convergence of iteration methods," *USSR Comput. Math. & Math. Phys.*, vol. 4, no. 5, pp. 1–17, 1964.
- [2] Y. Nesterov, "A method for solving the convex programming problem with convergence rate $O(1/k^2)$," in *Dokl. Akad. Nauk SSSR*, vol. 27, 1983, pp. 543–547.
- [3] Y. Nesterov, "Gradient methods for minimizing composite objective functions," *Math. Program.*, vol. 140, no. 1, pp. 125–161, 2013.
- [4] L. Bottou and Y. Le Cun, "On-line learning for very large data sets," *Appl. Stoch. Models Bus. Ind.*, vol. 21, no. 2, pp. 137–151, 2005.
- [5] A. Beck and M. Teboulle, "A fast iterative shrinkage-thresholding algorithm for linear inverse problems," *SIAM J. Imaging Sci.*, vol. 2, no. 1, pp. 183–202, 2009.
- [6] M. Hong, M. Razaviyayn, Z.-Q. Luo, and J.-S. Pang, "A unified algorithmic framework for block-structured optimization involving big data: With applications in machine learning and signal processing," *IEEE Signal Process. Mag.*, vol. 33, no. 1, pp. 57–77, 2016.
- [7] A. Badithela and P. Seiler, "Analysis of the heavy-ball algorithm using integral quadratic constraints," in *Proceedings of the 2019 American Control Conference*, 2019, pp. 4081–4085.
- [8] I. Sutskever, J. Martens, G. Dahl, and G. Hinton, "On the importance of initialization and momentum in deep learning," in *Proc. ICML*, 2013, pp. 1139–1147.
- [9] Y. Nesterov, *Lectures on convex optimization*. Springer Optimization and Its Applications, 2018, vol. 137.
- [10] L. Lessard, B. Recht, and A. Packard, "Analysis and design of optimization algorithms via integral quadratic constraints," *SIAM J. Optim.*, vol. 26, no. 1, pp. 57–95, 2016.
- [11] S. Cyrus, B. Hu, B. Van Scoy, and L. Lessard, "A robust accelerated optimization algorithm for strongly convex functions," in *Proceedings of the 2018 American Control Conference*, 2018, pp. 1376–1381.
- [12] B. V. Scoy, R. A. Freeman, and K. M. Lynch, "The fastest known globally convergent first-order method for minimizing strongly convex functions," *IEEE Control Syst. Lett.*, vol. 2, no. 1, pp. 49–54, 2018.
- [13] D. Maclaurin, D. Duvenaud, and R. Adams, "Gradient-based hyperparameter optimization through reversible learning," in *Proc. ICML*, 2015, pp. 2113–2122.
- [14] Y. Bengio, "Gradient-based optimization of hyperparameters," *Neural Comput.*, vol. 12, no. 8, pp. 1889–1900, 2000.
- [15] A. Beirami, M. Razaviyayn, S. Shahrampour, and V. Tarokh, "On optimal generalizability in parametric learning," in *Proc. Neural Information Processing (NIPS)*, 2017, pp. 3458–3468.
- [16] Z.-Q. Luo and P. Tseng, "Error bounds and convergence analysis of feasible descent methods: a general approach," *Ann. Oper. Res.*, vol. 46, no. 1, pp. 157–178, 1993.
- [17] H. Robbins and S. Monro, "A stochastic approximation method," *Ann. Math. Statist.*, pp. 400–407, 1951.
- [18] A. Nemirovski, A. Juditsky, G. Lan, and A. Shapiro, "Robust stochastic approximation approach to stochastic programming," *SIAM J. Optim.*, vol. 19, no. 4, pp. 1574–1609, 2009.
- [19] O. Devolder, "Exactness, inexactness and stochasticity in first-order methods for large-scale convex optimization," Ph.D. dissertation, Louvain-la-Neuve, 2013.
- [20] P. Dvurechensky and A. Gasnikov, "Stochastic intermediate gradient method for convex problems with stochastic inexact oracle," *J. Optimiz. Theory App.*, vol. 171, no. 1, pp. 121–145, 2016.
- [21] H. Mohammadi, M. Razaviyayn, and M. R. Jovanović, "Robustness of accelerated first-order algorithms for strongly convex optimization problems," *IEEE Trans. Automat. Control*, vol. 66, no. 6, pp. 2480–2495, 2021.
- [22] B. O'Donoghue and E. Candes, "Adaptive restart for accelerated gradient schemes," *Found. Comput. Math.*, vol. 15, pp. 715–732, 2015.
- [23] H. Mohammadi, S. Samuelson, and M. R. Jovanović, "Transient growth of accelerated optimization algorithms," *IEEE Trans. Automat. Control*, 2022, doi:10.1109/TAC.2022.3162154; also arXiv:2103.08017.
- [24] N. S. Aybat, A. Fallah, M. M. Gürbüzbalaban, and A. Ozdaglar, "Robust accelerated gradient methods for smooth strongly convex functions," *SIAM J. Opt.*, vol. 30, no. 1, pp. 717–751, 2020.
- [25] B. V. Scoy and L. Lessard, "The speed-robustness trade-off for first-order methods with additive gradient noise," 2021, arXiv:2109.05059.
- [26] Y. Nesterov, *Introductory lectures on convex optimization: A basic course*. Springer Science & Business Media, 2004, vol. 87.
- [27] M. Muehlebach and M. Jordan, "A dynamical systems perspective on Nesterov acceleration," in *International Conference on Machine Learning*. PMLR, 2019, pp. 4656–4662.
- [28] H. Kwakernaak and R. Sivan, *Linear optimal control systems*. Wiley-Interscience, 1972.
- [29] K. Ogata, *Discrete-time control systems*. New Jersey: Prentice-Hall, 1994.